THE UNIVERSITY OF ALBERTA

AN EXPLORATORY STUDY OF STORMWATER DROPSHAFTS

by

© LARRY SIU-KUEN FUNG

A THESIS

SUBMITTED TO THE FACULTY OF GRADUATE STUDIES AND RESEARCH

IN PARTIAL FULFILMENT OF THE REQUIREMENTS FOR THE DEGREE

OF MASTER OF SCIENCE

THE DEPARTMENT OF CIVIL ENGINEERING

EDMONTON, ALBERTA

FALL 1983

Abstract

This thesis is a result of part 1 of a 2 part research project initiated by the City of Edmonton Water and Sanitation Department. The objective of the first part of the study is to provide a theoretical evaluation of the two types of drop structures used in the City, and to provide recommendations for the improvement of their design practice, as well as further studies (part 2) to answer outstanding questions.

These structures are called the shaft drop structures and the drill drop structures primarily due the different methods of construction. They are analysed by dividing the structures into identifiable hydraulic components. Discussions and analyses include the hydraulics of various elements of the structures, the possible flow types and controls, balance sizing of the components, the aeration problem, and the surcharge conditions. Wherever possible, theoretical derivations are verified with published data or with some new experiments in the laboratory.

Based on the analysis, criteria for evaluating the hydraulic performance of these structures are provided. Modifications and improvements are also suggested. Further experimental studies are recommended to tie-in with the theory and to develop adequate design procedures for these structures.

Acknowledgements

The author would like to sincerely thank Dr. N. Rajaratnam and Prof. A. W. Peterson for their encouragement and guidance throughout the course of this study.

The aid of Messrs. S. Lovell and J. Gagne in constructing and maintaining the experimental apparatus is greatly appreciated. Discussions with Messr. G. A. Kercher, providing the practical aspects of the problem, is also acknowledged. Financial support for the study was provided by the Edmonton Water and Sanitation Department and supplemented by the Natural Science and Engineering Research Council through grants to Dr. N. Rajaratnam and Prof. A.W. Peterson. These are gratefully acknowledged.

Finally, the author would like to thank his wife, Susanne, whose support and patience have made the completion of the study possible.

Table of Contents

List of Tables

List of Figures

List of Symbols

A	flow area
a	subscript for air or atmospheric
b	nappe width
c	subscript for critical flow section
C_d	drag coefficient
C_f	friction coefficient
C_m	air concentration in fully developed flow
d	nappe thickness
D	diameter of pipe or shaft
e	subscript for end section
f	subscript for friction
f	function
f'	friction factors
F_f	back pressure force
F	Froude number
g	gravitational acceleration, or subscript for gas
H	entrance transition height, or height of water fall, or depth in head chamber
H_n	head loss
H_{ns}	head losses in drop shaft
h	length of drop shaft from inlet invert to outlet invert
H_s	submerged length of shaft
i	subscript for inner
J	volumetric flux
j	subscript for total volumetric flux

K	coefficient
K_1	pressure coefficient
K_e	exit loss coefficient
K_o	entrance loss coefficient
L_r	length of roller at shaft entrance
L_{rj}	length of roller of hydraulic jump
L	length of outlet sewer
L_d	disintegration length
M	momentum flux
M	*m*ass flux
$_m$	subscript for average
$_o$	subscript for outlet
P	pressure at a section, or wetted perimeter
P_d	drag force
q	discharge per unit width
Q	discharge
Q_θ	discharge into a sector of inscribed angle θ
R	radius of shaft
r	radius
S_c	critical slope
S_o	bed slope
$_s$	subscript for side
T_z	tailwater depth
$_t$	subscript for total
V	average velocity at a section
V_d	full-flow velocity
V_o	incipient entrainment velocity

V_{o_t}	average outlet velocity
V_2	velocity of flow as it arrives at the plunge pool
V_{gj}	drift velocity of gas relative to the volumetric average
v	subscript for vertical, or velocity at a point
W	weight of fluid element
w	subscript for water
x	subscript for the horizontal direction
X_o	length of forced hydraulic jump
y	depth of flow
y_c	critical depth
y_e	end depth
$\bar{y}$	depth of center of gravity below free surface
y_o	flow depth in the outlet sewer
y_{o_t}	minimum outlet depth
y_2	subcritical sequent depth
y_3	supercritical flow depth in basin
Δh	step height of plunge pool
Δz	vertical distance between the invert of inlet and the mid-depth of the flow section in front of the roller
α	angle of sewer invert to the horizontal or void fraction
β	$\Delta h/y_3$ or momentum coefficient
β_a	ratio of air discharge to water discharge
ψ	function of y/D
ψ_a	y_o/y_2

λ	function of y/D
γ	specific weight of fluid
Λ	βC_d
ϕ	y_2/y_3
σ	surface tension
μ	absolute viscosity
θ	angle of impingement, or inscribed angle of a sector
*	superscript for dimensionless quantities
ϵ	turbulent intensity
ρ	density

1. Introduction

1.1 Background

In a municipal sewer system, drop structures are used to disharge wastewater from a higher elevation to a lower elevation. They may be required for a variety of reasons. Typically, for development in a high relief area, drops are required to absorbed extra head losses so as to maintain sewers at an acceptable grade. For the discharge of stormwater directly into the river located in an entrenched valley with steep valley walls, drops are required to connect the sewer elevation to the river elevation. Also, for old municipality, the development of underground storage tunnels for the temporary storage of excess stormwater during flood peak means the requirement of drops to connect the sewer system to the storage tunnels underneath.

The second example listed above is typical of the riverbank area in Edmonton, whereas the last example describes the situation in Chicago. Usually, vertical drops are used due to the limitation of space, and cost of construction. In Edmonton, two types of drop structures are in use. They are the shaft drop structures and the drill drop structures. Their typical geometries are shown in Fig. 1 and Fig. 2.

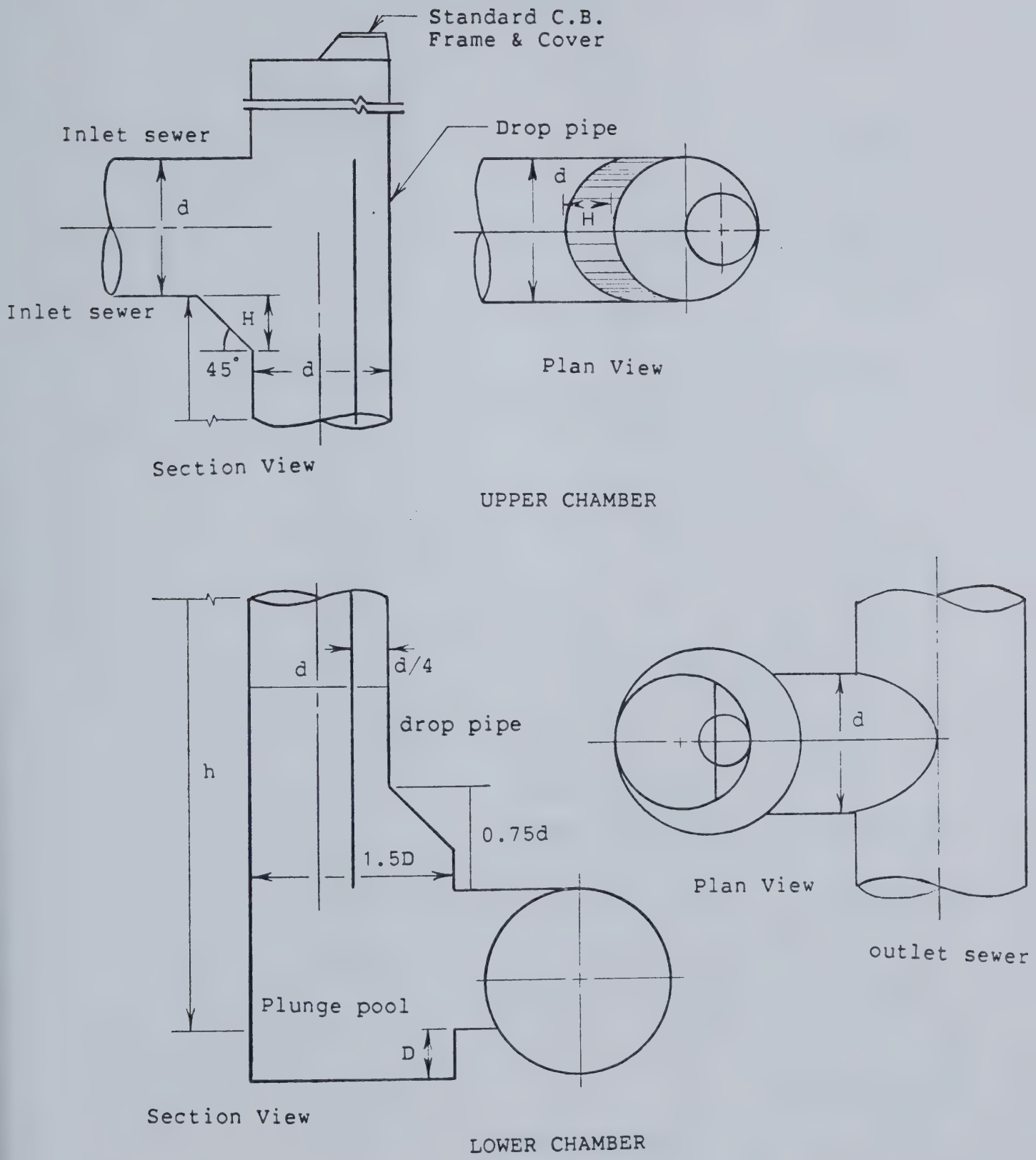

Fig. 1 - Geometry of shaft drop structures

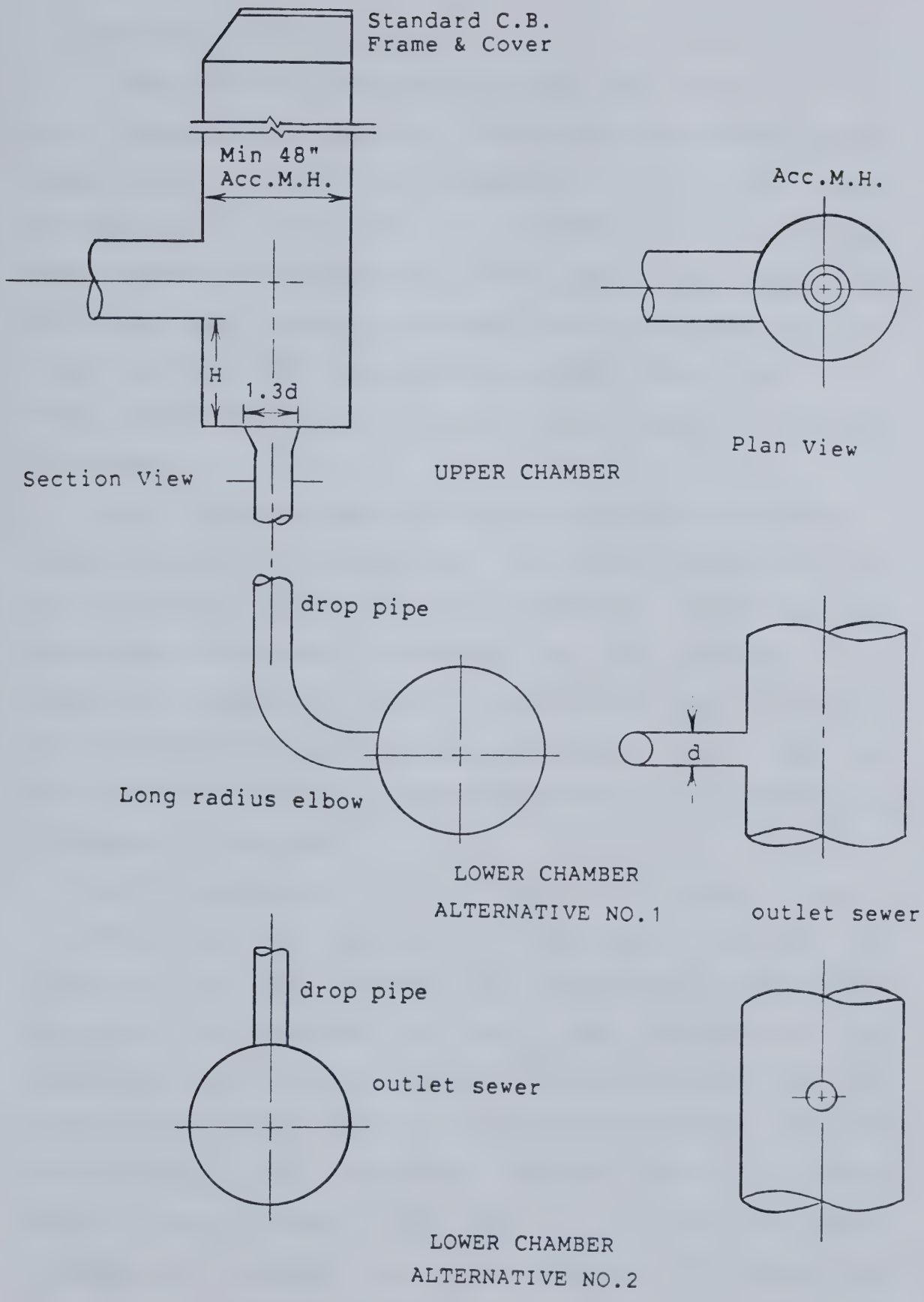

Fig. 2 - Geometry of drill drop structures

1.2 Outline of Presentation

The shaft drop structures and the drill drop structures are discussed individually. The shaft drop structure can be subdivided into three major components: 1) the inlet sewer and the shaft entrance; 2) the drop shaft; and 3) the plunge pool and the entrance to the outlet sewer. The drill drop structure can also be subdivided into three components: 1) the inlet sewer; 2) the entrance chamber; and 3) the drill drop pipe. The hydraulics of each component will be discussed .

The various types of flow controls which may exist in this structures are presented. Theoretical development of the governing equations for these flow types and the conditions for their existence is also provided where possible. A computer program for the evaluation of the drill drop structures is also included bearing in mind that its development is based on the assumptions and approximations discussed in the text.

Air entrainment in drop shafts has been an active research area for the last twenty years. Due to the complexity of the problem, no comprehensive theoretical treatment is available at this time. Furthermore, its dependence on viscous and surface tension effects has made modelling extremely difficult. Based on recent research developments, some modelling criteria are now available. However, many problems have yet to be resolved before satisfactory models can be developed. For practical

purposes, empirical relations for air demand may be developed based on field observations.

Overloading, in terms of exceeding the design capacity and maximum tailwater level, is also discussed. Other associated problems, such as erosion due to high velocity, cavitation, impact pressure at the base of drop shaft, and the hydrostatic uplift pressure due to high groundwater table, are also included.

Based on the theoretical discussions, some possible modifications are suggested for consideration to improve the hydraulic efficiency of such structures. Recommendations for future experimental studies are also provided.

2. Shaft Drop Structures

2.1 Inlet Sewer

2.1.1 Discharge Capacity

The discharge capacity of the inlet sewer may be determined with simple culvert hydraulics. In general, the discharge and depth in a sewer can be described by the following relation,

$$y/D = f\ (\ Q/g^{1/2}D^{5/2},\ S,\ f'\ ) \qquad (1)$$

where y is the normal depth, Q is the discharge, S is the slope of the invert, D is the diameter, and f' is the friction factor. In particular, the critical depth and discharge are uniquely related and can be written as,

$$y_c/D = f_1\ (\ Q/g^{1/2}D^{5/2}\ ) \qquad (2)$$

A culvert may have inlet control, outlet control, or pipe-flow control, depending on the slope, length, entrance condition, and the tailwater level. A definition sketch of these is shown in Fig. 3. In a normal design situation, the discharge capacity and allowable head water-level are predetermined. The allowable slope is determined by site conditions and other sanitary constraints. If the capacity of the vertical shaft is designed so that backup at the shaft-entrance will not occur, and if the sewer slope is mild, critical depth control at the oulet will always exist.

One method of solving for the appropriate inlet size is to use a trial-and-error procedure. First of all, a trial

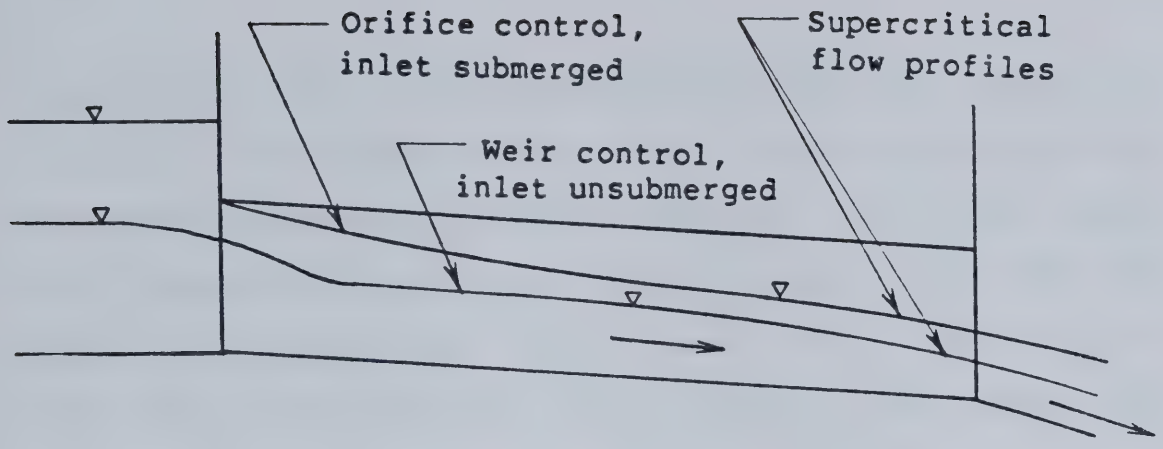

(A) Inlet control, sewer is short and steep

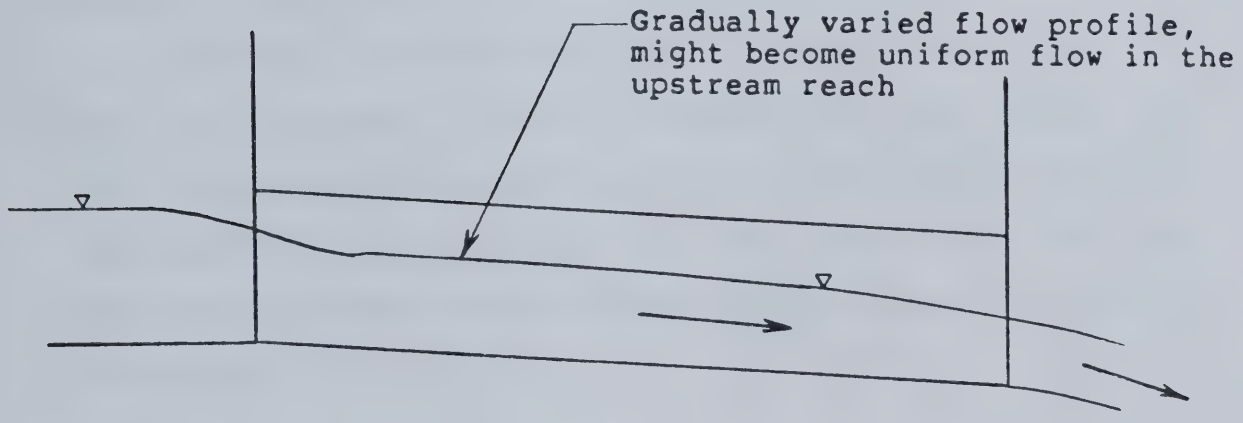

(B) Outlet control when the outlet is unsubmerged; sewer slope is mild

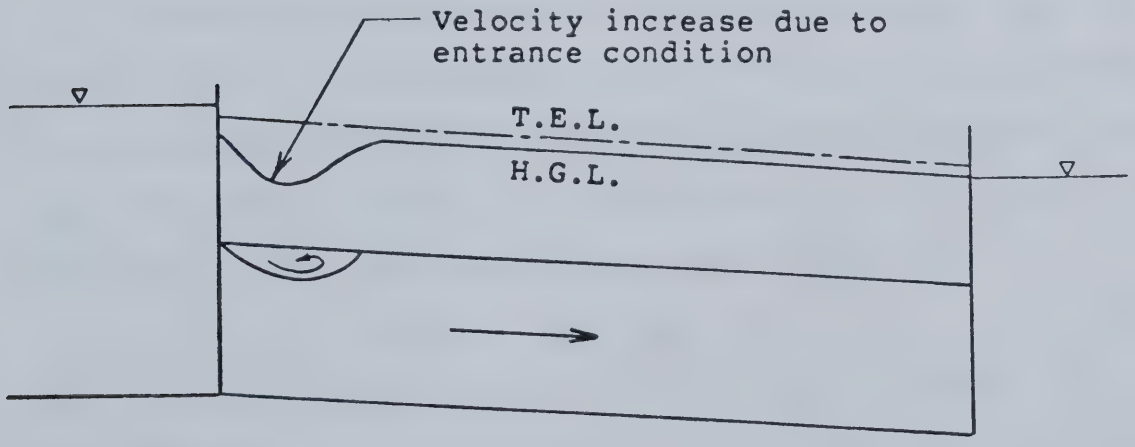

(C) Pipe flow control when both the inlet and the outlet are submerged

Figure 3 - Definition sketch of the inlet flow controls

pipe size is selected and the critical depth for the design discharge is computed. Then, the flow depths at various locations of the pipe are determined by a gradually varied flow computation, starting at the critical section near the outlet to a section just behind the inlet. The headpool water-level may be calculated by taking into account the entrance head loss. If it is different from the required headpool level, a new pipe size will be chosen and the procedure repeated.

According to Henderson(1966), a culvert will flow full when y_c/D is greater than 0.9, except near the brink. In this case, the discharge capacity may be computed using the full-pipe-flow equation with the head equal to the head difference between the headpool and the center line of the sewer outlet.

2.1.2 Momentum Considerations

If the inlet flow goes through critical depth near the shaft entrance, the discharge in the inlet may be determined by the momentum equation between the critical section and the end depth section as discussed by Rajaratnam and Muralidhar(1964). The equation can be written as:

$$P - P_e + W\sin\alpha - P_f = M_e - M \qquad (3)$$

where P is the total pressure at the critical section, P_e is the pressure at the end section, W is the weight of fluid between the two sections, α is the angle of the pipe invert to the horizontal, P_f is the boundary friction force, M_e is

the momentum flux at the end section, and M is the momentum flux at the critical section.

For small sewer slopes and short control volume length, the term ($W\sin\alpha - P_f$) is small compared to the pressure and momentum terms, hence,

$$P - P_e = M_e - M \tag{4}$$

wherein $$P = \gamma \bar{y} A \cos\alpha, \tag{5}$$

$$P_e = \gamma \bar{y}_e A_e K_1 \cos\alpha, \tag{6}$$

$$M = \frac{\gamma Q^2}{g} \cdot \frac{1}{A} \cdot \beta, \tag{7}$$

and $$M_e = \frac{\gamma Q^2}{g} \cdot \frac{1}{A_e} \cdot \beta \tag{8}$$

where $\bar{y}$ is the depth from the water surface to the centre of gravity of the section, A and A_e are the cross-sectional areas for the respective sections, and β is the momentum coefficient.

By substituting (5), (6), (7), and (8) into (4), and putting $\cos\alpha \simeq 1$ for small invert slope, (4) can be changed into:

$$\psi_c D^2 \lambda_c y_c - K_1 \psi_e D^2 \lambda_e y_e = \frac{Q^2}{g}\left[\frac{1}{\psi_e D^2} - \frac{1}{\psi_c D^2} \right] \tag{9}$$

where $A = \psi D^2$, and $\psi = f_3(y/D)$ (10)

and $\bar{y} = \lambda y$, and $\lambda = f_4(y/D)$ (11)

wherein ψ and λ are dimensionless coefficients and are unique functions of y/D, K_1 is the pressure coefficient at the end section, A is the area, $\bar{y}$ is the depth of the centre of gravity below free surface, y_c is the critical depth, y_e is the end depth, and, c and e stand for the critical

section and the end section respectively. For the critical discharge,

$$\frac{Q^2}{g} = \frac{1}{2} \cdot \frac{\psi_c^2 D^5}{\sqrt{\frac{y_c}{D} - \left[\frac{y_c}{D}\right]^2}} \qquad (12)$$

From the experiments of Rajaratnam and Muralidhar(1964), $y_e/y_c \simeq 0.725$ for $0 \leq y_c/D \leq 0.9$ and a horizontal pipe. Also, K_1 is a function of S_o/S_c only, and for a pipe slope of zero, K_1 is zero. The variations of y_e/y_c and K_1 with S_o/S_c are shown in Fig. 4 and Fig. 5. If the discharge in the inlet sewer is known, the critical depth and the end depth at the shaft entrance can be computed. Combining (9) and (12) gives:

$$P_c^* - K_1 P_e^* = \left[\frac{Q}{\sqrt{g} D^{2.5}}\right]^2 \cdot \left[\frac{1}{\psi_e} - \frac{1}{\psi_c}\right] \qquad (13)$$

where $P_c^* = A_c \bar{y}_c / D^3$

and $P_e^* = A_e \bar{y}_e / D^3$

Putting $Q^* = Q/g^{1/2} D^{5/2}$, we get:

$$Q^* = \left[\frac{P_c^* - K_1 P_e^*}{(1/\psi_e - 1/\psi_c)}\right]^{1/2} \qquad (14)$$

Values of P_c^*, P_e^*, ψ_c , and ψ_e may be obtained from Appendix I.

2.1.3 Shaft Entrance Conditions

Unless a smooth vertical curve is provided, the lower nappe will not follow the inlet boundary. Instead, it will leave the invert to strike the vertical shaft wall. A

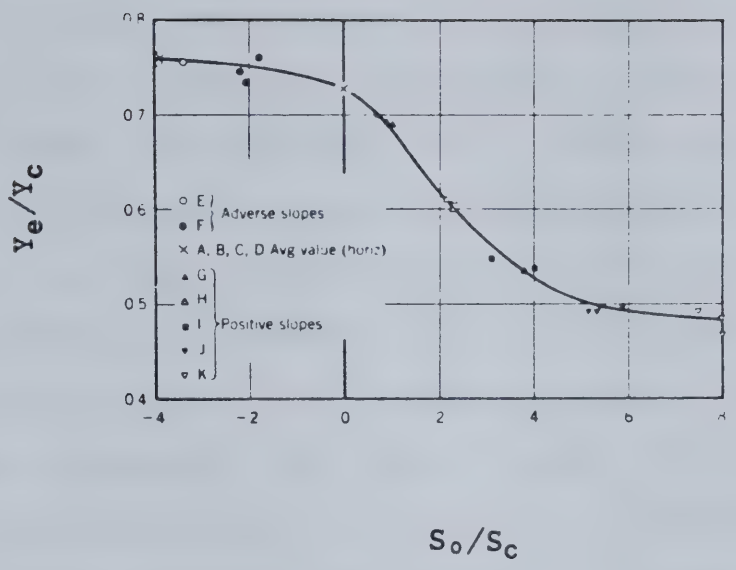

Figure 4 - End depth ratio for circular channels (From Rajaratnam and Muralidhar(1964))

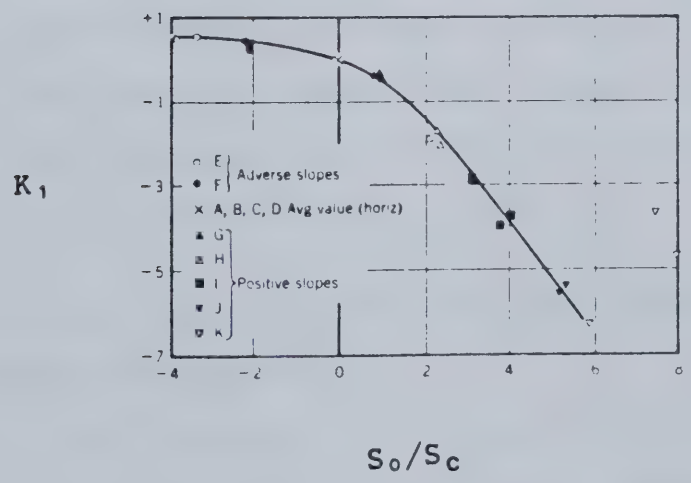

Figure 5 - Pressure coefficient K_1 for circular channels (From Rajaratnam and Muralidhar(1964))

surface roller will form on the upper nappe which entrains air[1]. Part of the entrained air will be carried down the shaft giving the downward flow a foamy-white appearance. If air is not allowed into the upper air chamber or the rate of air inflow is less than that of evacuation, it may be drawn in from the upstream manhole. The pressure in the air pocket above the upper nappe will then be somewhat subatmospheric. If adequate ventilation is designed for and maintained during operation, air pressure above the nappe will be almost atmospheric and the air supply will not be a problem.

Without a model analysis, it is difficult to predict as to whether the nappe will separate the upper and lower air chambers. For the moment, if separation is assumed to be possible when the drop shaft size is the same as the inlet size, and when the y_e/D ratio is greater than 0.5, then there can be two main categories of flow: one in which the upper and lower air chambers are connected, and the other in which they are separated. A definition sketch of the flow at the shaft entrance is shown in Fig. 6.

2.1.3.1 Flow Conditions When the Flow Separates the Upper and Lower Air-chambers

In this situation, the upper air chamber above the nappe is vented by the manhole at ground level, while the lower chamber is ventilated by the outlet. If the outlet remains open and is ventilated, the downward flow will be an

---

[1] Air entrainment by a surface roller due to impingement has been summarized by Rao and Kobus(1974), and will be discussed in a later section on air entrainment.

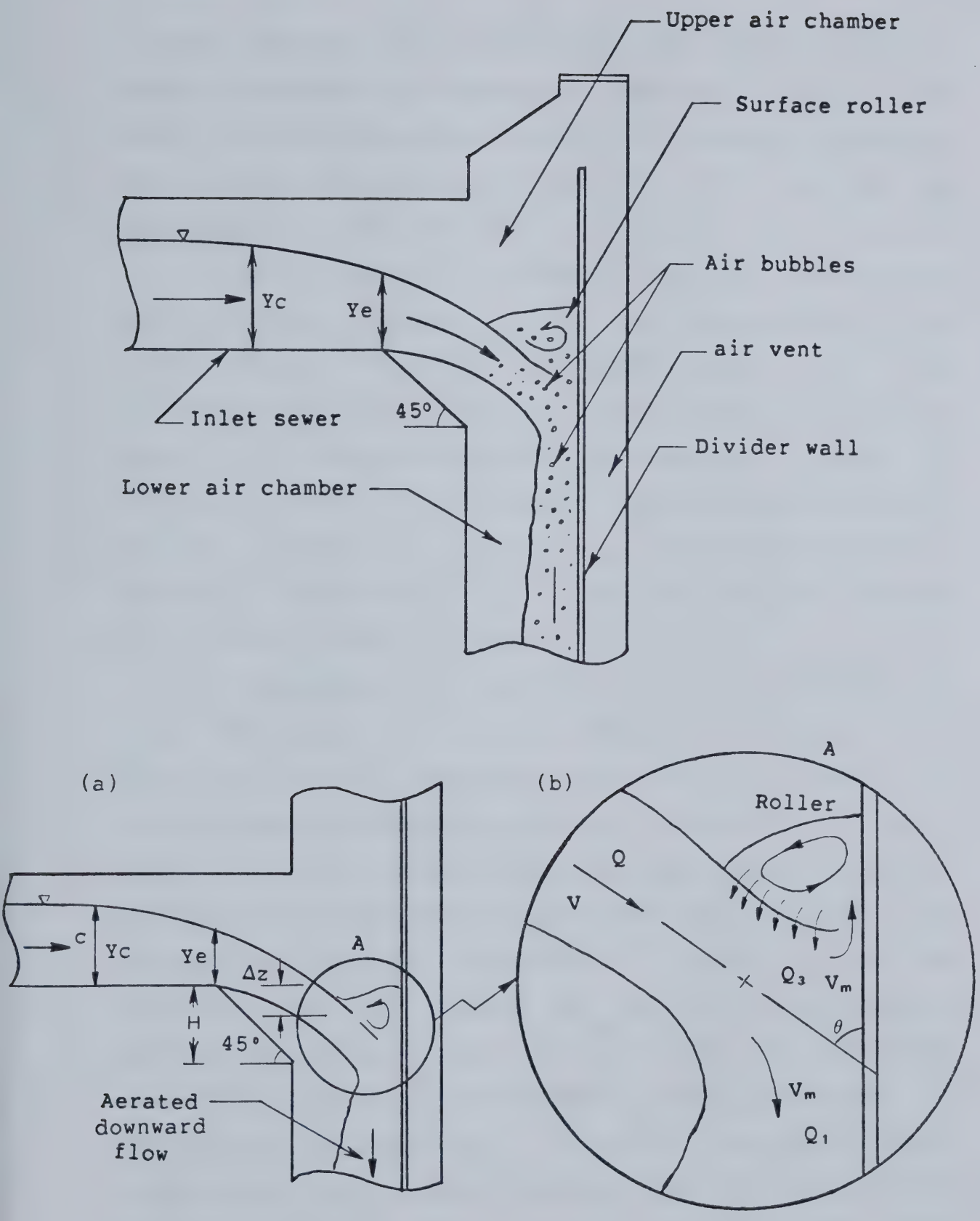

Figure 6 - Definition sketch of the flow at the shaft entrance

aerated vertical flow. Since the pressure in the shaft remains approximately atmospheric, the energy balance in the shaft is generally assumed to obey the Bernoulli criterion. The air entrainment aspects of this type of flow will be discussed in a later section.

If the drop shaft is lengthened such that the expanding downward flow eventually fills the cross-section of the shaft before it reaches the outlet, due to the air entraining capacity of the flow, it is possible that the air pocket in the shaft may gradually be evacuated, forming an air-water mixture in the shaft. One-dimensional two-phase flow in a vertical pipe has been analysed by Wallis(1969). A summary of the derivation of the momentum equation, together with a worked example is shown in section 2.2.

A homogeneous two-phase flow is probably not a steady state phenomenon in an open dropshaft system. Once substantial negative pressure is developed in the shaft, air will probably be forced into the shaft through the entrance. This is a well known phenomenon which was described by Blaisdell(1958,1952) as air-controlled flow. The flow is characterized by the formation of a noisy air core. The velocity of air will depend on the pressure difference between the entrance and the dropshaft, and can differ significantly from the fluid velocity. The insufflation of air may be intermittent or continuous and cause violent vibration of the structure. The method of analysis of this flow is uncertain. The two-phase flow theory might apply

just below the entrance with the negative pressure relieved by the air insufflation which gradually diffuses into the flow. The flow may even separate from the pipe wall as it accelerates down the shaft, and will thus be ventilated by the outlet. Further experimental work is needed to clarify these comments.

2.1.3.2 Flow Conditions When the Flow Does Not Separate the Upper and Lower Air-chambers

This flow type will occur when y_e/D is less than 0.5. The pressure in the lower air-chamber will be atmospheric since it is ventilated. Because the air-supply in the dropshaft is not a problem, the flow in the shaft will be a free-entraining self-aerated flow. Its analysis is similar to the previous case where the lower air chamber is ventilated by the outlet and will be discussed in a later section.

2.1.3.3 Possibility of Orifice Flow

Orifice flow is a quiescent stage of flow with the entrance flowing full and approximately level. Inside the pipe, the flow goes through a contraction with very little to no air entrainment from the inlet, and remains partly full throughout the pipe length. The annular air space is continuous and open to the outlet. This type of flow is highly inefficient because the discharge capacity of the pipe is greatly reduced with respect to the available head at the entrance.

Therefore, the entrance should be designed in such a way that orifice control will not govern the flow. Orifice flow may be suppressed by one of the following ways: 1) enlarging the entrance; 2) providing a smooth inlet; or 3) insuring that the length of the vertical pipe is long enough so that the expanding flow will be capable of evacuating the air pocket in the shaft if orifice flow does occur. Experiments done by Anderson and Dahlin(1975) for the Tunnel And Reservoir Project (TARP) in Chicago showed that if the entrance to the shaft is a smooth elbow, the nappe will always follow the inner pipe boundary, and hence weir flow will always occur.

Although the entrance in the present case is not smooth, it is uncertain whether orifice flow would occur. Since the form of flow control is strongly dependent on the geometry of the inlet, it is advisable to use a smooth transition.

2.1.3.4 Entrance Hydraulics

Referring to Fig. 6, if we write the Bernoulli equation between section c and a section in front of the roller, we have:

$$y_c + V_c^2/2g + \Delta z = V^2/2g + H_n \qquad (15)$$

where V_c is the critical velocity, Δz is the vertical distance between the invert of inlet and the mid-depth of the flow section in front of the roller, V is the velocity in front of the roller, and H_n is the head loss between the two sections.

The surface roller above the upper nappe will reduce the kinetic energy of the flow somewhat. If the velocity of the downward flow after impingement is V_m, the vertical component of the momentum equation for the impingement region can be written as:

$$\rho Q_1 V_m(1-\cos\theta) = \rho Q_3 V_m(1+\cos\theta) \tag{16}$$

or

$$\frac{Q_3}{Q_1} = \frac{1 - \cos\theta}{1 + \cos\theta} \tag{17}$$

where Q_1, Q_3, and θ are defined in Fig. 6. Also, for the impingement region:

$$\rho QV = \rho Q_1 V_m + \rho Q_3 V_m \tag{18}$$

where V_m is the velocity just below the impingement region, and V is the velocity of the flow before entering the roller. Combining (17) and (18) and simplifying:

$$V_m = \frac{(\ 1 + \cos\theta\ )}{2} \cdot V \tag{19}$$

The momentum equation in the x direction is,

$$\gamma \bar{y}_c A_c + \rho QV_c = \rho QV_x \tag{20}$$

which may be rewritten as:

$$\frac{\lambda_c \psi_c y_c}{D} = \frac{Q}{gD^3} \cdot (\ V_x - V_c\ ) \tag{21}$$

The first term is a dimensionless pressure force term which is a unique function of y_c/D, and was defined earlier as P_c^* (see Appendix I). The critical velocity, V_c, is equal to $Q/\psi_c D^2$. Hence, (21) may be rewritten as:

$$V\sin\theta = \frac{gD^3 P_c^*}{Q} + \frac{Q}{\psi_c D^2} \tag{22}$$

Neglecting the head loss term in (15), substituting it into (22) and rearranging:

$$\sin\theta = \frac{\left[\frac{gD^3P_c^*}{Q} + \frac{Q}{\psi_c D^2} \right]}{\sqrt{2g\left(\Delta z + y_c + \frac{Q^2}{2gD^4\psi_c^2} \right)}} \tag{23}$$

Now, substitute (23) into (19):

$$V_m = \frac{1}{2}\left[1 + \sqrt{1 - \frac{\left[\frac{gD^3P_c^*}{Q} + \frac{Q}{\psi_c D^2} \right]^2}{2g\left(\Delta z + y_c + \frac{Q^2}{2gD^4\psi_c^2} \right)}} \right] * \left[\sqrt{2g\left(\Delta z + y_c + \frac{Q^2}{2gD^4\psi_c^2} \right)} \right] \tag{24}$$

The value of Δz should be obtained from experiments. With the lack of model observations, Δz may be assumed to be:

$$\Delta z = \frac{1}{2} \cdot g \left[\frac{D + H - L_r}{V_x} \right]^2 \tag{25}$$

where H is the entrance step height, and Lr is the length of the roller. Combining (21) and (25), and rearranging:

$$\Delta z = \frac{1}{2} \cdot g \cdot \frac{(D + H - L_r)^2}{\left[\frac{gD^3P_c^*}{Q} + \frac{Q}{\psi_c D^2} \right]^2} \tag{26}$$

If the discharge is known, the average velocity just below the entrance, V_m, can be computed.

2.2 Considerations for Flow of Air-water Mixture

2.2.1 Derivation of Momentum Equation

One dimensional two-phase flow theory was discussed by Wallis(1969). The derivation of the steady state momentum equation for an air-water flow in a vertical shaft is as follows:

Considering a section of the fluid in the vertical pipe as shown in Fig. 7, the momentum equation for the air-water mixture can be written as:

$$W\frac{dV}{dZ} = -A\frac{dp}{dZ} - P\tau_w - A\rho_m g \tag{27}$$

or

$$\frac{dp}{dZ} = -\frac{P}{A}\tau_w - \frac{W}{A}\cdot\frac{dV}{dZ} - \rho_m g \tag{28}$$

where W is the mixed mean mass flow rate of air and water, V is the mean velocity of the mixture within the element, Z is the direction of flow, P is the perimeter of the element in contact with the pipe wall, A is the cross-sectional area, τ_w is the average wall shear stress, p is the average pressure at a pipe cross-section, ρ_m is the average density of the mixture, and g is the gravitational acceleration.

The three terms on the right hand side of equation 28 can be rewritten as:

$$\frac{dp}{dZ} = +\left[\frac{dp}{dZ}\right]_F + \left[\frac{dp}{dZ}\right]_A + \left[\frac{dp}{dZ}\right]_G \tag{29}$$

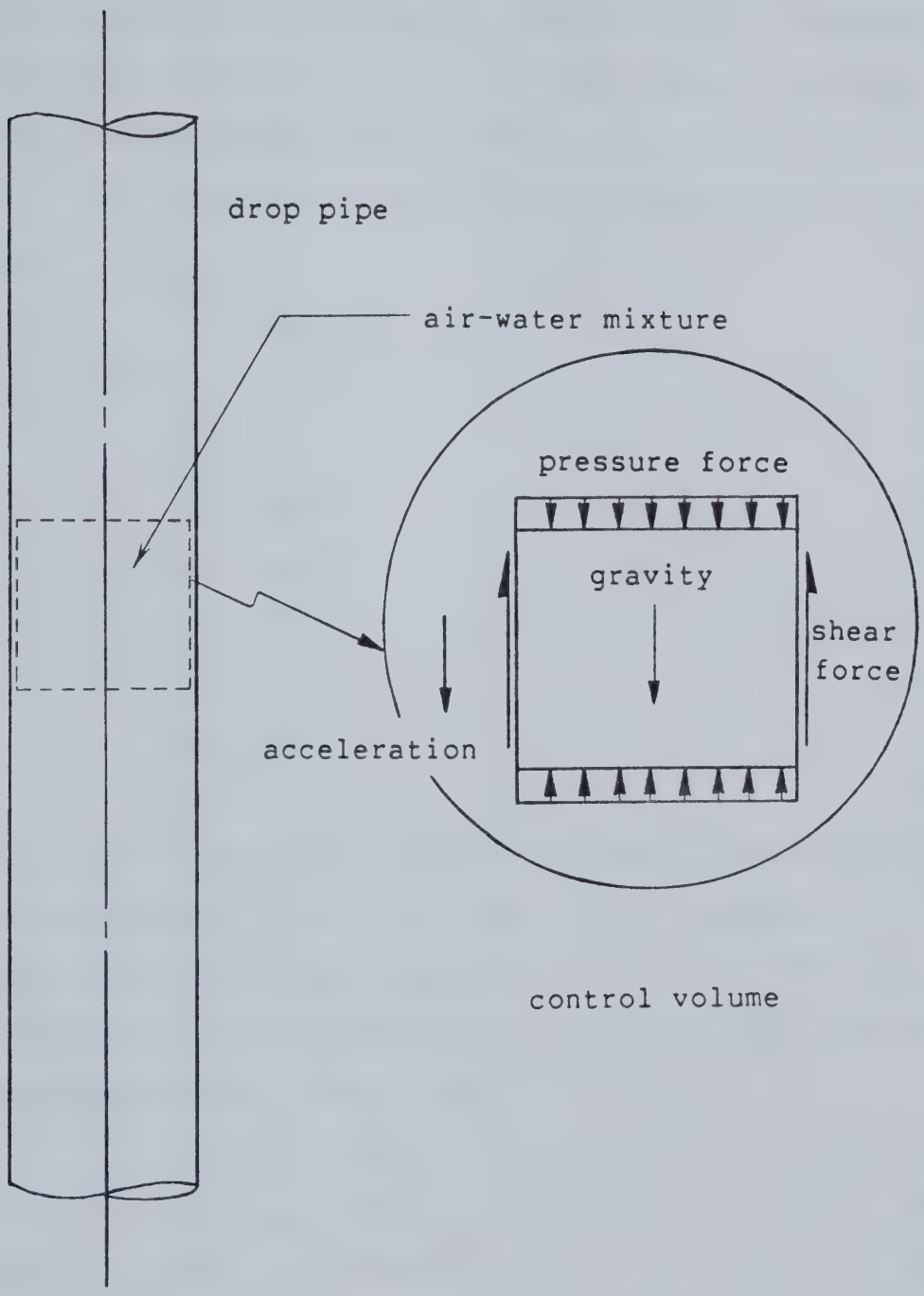

Fig. 7 - Momentum considerations of a cylindrical section in the vertical drop pipe

If J represents the volumetric flux which is the volumetric discharge divided by the cross-sectional area, Q is the volumetric discharge, V is the velocity, α refers to the volumetric fraction of air in the pipe, subscript w refers to water, subscript g refers to air, and subscript j refers to the total flux, the following expressions can be written:

$$J = J_w + J_g \tag{30}$$

$$V_g = J_g/\alpha \tag{31}$$

$$V_w = J_w/(1-\alpha) \tag{32}$$

$$J_w = Q_w/A \tag{33}$$

$$J_g = Q_g/A \tag{34}$$

$$V_{wj} = V_w - J \tag{35}$$

$$V_{gj} = V_g - J \tag{36}$$

$$J_{gj} = \alpha(V_g - J) \tag{37}$$

$$J_{wj} = (1 - \alpha)\cdot(V_w - J) \tag{38}$$

where V_{wj} is the drift velocity of water relative to the volumetric average, V_{gj} is the drift velocity of air relative to the volumetric average, J_{gj} is the drift flux of air relative to a surface moving at the average velocity, and similarly for J_{wj}. From (37),

$$\alpha J = \alpha V_g - J_{gj} \tag{39}$$

or $$\alpha J = J_g - \alpha V_{gj} \tag{40}$$

Therefore $$\alpha = J_g/(J + V_{gj}) \tag{41}$$

or $$\alpha = J_g/(J_w + J_g + V_{gj}) \tag{42}$$

Going back to (29),

$$-\left.\frac{dp}{dZ}\right|_A = M_g\frac{dV_g}{dZ} + M_w\frac{dV_w}{dZ} \tag{43}$$

where M_g is the air mass discharge rate per unit area, M_w is the fluid mass flow rate per unit area. Hence,

$$M_g = \rho_g Q_g/A \tag{44}$$

$$M_w = \rho_w Q_w/A \tag{45}$$

Substituting (42) into (31),

$$V_g = J_w + J_g + V_{gj} \tag{46}$$

Substituting (42) into (32),

$$V_w = \frac{J_w\cdot(\ J_w+J_g+V_{gj}\ )}{(\ J_w+V_{gj}\ )} \tag{47}$$

Since water is incompressible compared to air, J_w is constant down the shaft, hence, if we differentiate (46) and (47),

$$\frac{dV_g}{dZ} = \frac{dJ_g}{dZ} \tag{48}$$

$$\frac{dV_w}{dZ} = \frac{dJ_g}{dZ}\left[\frac{J_w}{J_w+V_{gj}}\right] \tag{49}$$

Also assuming isothermal expansion,

$$J_g = (\ P_{atm}\ /P\ )*(J_g)_{atm} \tag{50}$$

Differentiating,

$$\frac{dJ_g}{dZ} = -(J_g)_{atm}\cdot\frac{P_{atm}}{P^2}\cdot\frac{dP}{dZ} \tag{51}$$

Substituting (48) and (49) into (43),

$$-\left.\frac{dP}{dZ}\right|_A = \left[\ M_g+M_w\frac{J_w}{(\ J_w+V_{gj}\ )}\ \right]\cdot\frac{dJ_g}{dZ} \tag{52}$$

Substituting (51) into (52),

$$\left.\frac{dP}{dZ}\right|_A = \left[M_g + M_w \frac{J_w}{(J_w + V_{gj})} \right] \cdot (J_g)_{atm} \cdot \frac{P_{atm}}{P^2} \cdot \frac{dP}{dZ} \qquad (53)$$

For the frictional component,

$$-\left.\frac{dP}{dZ}\right|_F = \frac{2C_f MJ}{D} \qquad (54)$$

where C_f is the friction factor, M is the total mass flow rate per unit area, and J is the total volumetric flux, and D is the pipe diameter. For the gravity component,

$$-dP/dZ)_G = g\rho_m \qquad (55)$$

But $$\rho_m = \alpha\rho_g + (1-\alpha)\rho_w \qquad (56)$$

Hence, $$-(dP/dZ)_G = g(\alpha\rho_g + (1-\alpha)\rho_w) \qquad (57)$$

Substituting (53), (54), (57)into (29), we get:

$$-\frac{dP}{dZ} = \frac{2C_f MJ/D + g[\alpha\rho_g + (1-\alpha)\rho_w]}{1-[M_g + M_w J_w/(J_w + V_{gj})] * (J_g)_{atm} P_{atm}/P^2} \qquad (58)$$

This is the one-dimensional momentum equation for the two-phase flow in a vertical pipe.

2.2.2 Comparison with Anderson et. al.'s Data

Anderson, Vaidyaraman, and Chu(1971) had done some observations on the air-water flow problem in a vertical drop conduits. They found that the injection of air into the pipe is extremely effective in suppressing cavitation. In order to compare the analytical derivation with the published data of Anderson et. al., equation 58 is used to

predict the variation of pressure and velocity. These are compared with the actual measurements as shown in table 1. The pressure heads versus elevations are plotted on Fig. 8 for visual comparison.

The simplified homogeneous two-phase flow theory agrees well with the experimental data presented by Anderson, Vaidyaraman, and Chu. The application of the theory to prototype drop shaft is very limited due to unknown boundary conditions at the inlet and the assumption of homogeneity. In prototype drop shafts, free surface aeration will probably be the dominant inlet condition, which is again dependent on the inlet geometry. The outlet pressure will be at or above atmospheric depending on backwater condition.

The two-phase analysis is valid for the experimental situation by Anderson et. al. because a valved inlet controls the head loss and is thus closed to the atmosphere. The head chamber level is substantially above the inlet so that the drop pipe is forced to flow full. Air is allowed to enter the drop pipe through air vents evenly distributed at one elevation. Thus the rate of air inflow can be controlled as related to water discharge and becomes an independent variable. However, most prototype drop shafts have open inlets and a relatively small and shallow chambers. Hence, air flow rate depends on water discharge as well as inlet geometry. Flow types become considerably more complicated and the homogeneous air-water flow condition is very unlikely.

Table 1

Worked example

z (m)	Δz (m)	α	P_1 (kPa)	Jg (m/s)	Jw (m/s)	J (m/s)	Vg (m/s)	Vw (m/s)	P_2 (kPa)
0.0	0.0	0.377	101.3	1.539	2.794	4.333	4.803	4.484	101.3
1.06	-1.058	0.391	95.6	1.631	2.794	4.424	4.174	4.585	103.7
2.37	-1.317	0.409	88.6	1.759	2.794	4.552	4.302	4.725	88.5
3.70	-1.329	0.428	81.8	1.905	2.794	4.698	4.448	4.886	80.5
4.97	-1.272	0.448	75.5	2.063	2.794	4.857	4.607	5.060	75.5
6.40	-1.421	0.471	68.8	2.266	2.794	5.060	4.810	5.282	68.9
7.66	-1.269	0.493	63.0	2.473	2.794	5.267	5.017	5.510	61.2
8.47	-0.808	0.507	59.5	2.619	2.794	5.412	5.162	5.670	60.7
8.92	-0.451	0.515	57.6	2.705	2.794	5.499	5.249	5.765	58.6
9.39	-0.468	0.524	55.7	2.799	2.794	5.593	5.343	5.868	59.4
9.85	-0.460	0.532	53.8	2.897	2.794	5.690	5.440	5.975	58.5
10.3	-0.458	0.541	52.0	2.999	2.794	5.793	5.543	5.087	58.8

P_1 is the calculated pressure

P_2 is the measured pressure

These pressures are plotted in Fig. 8

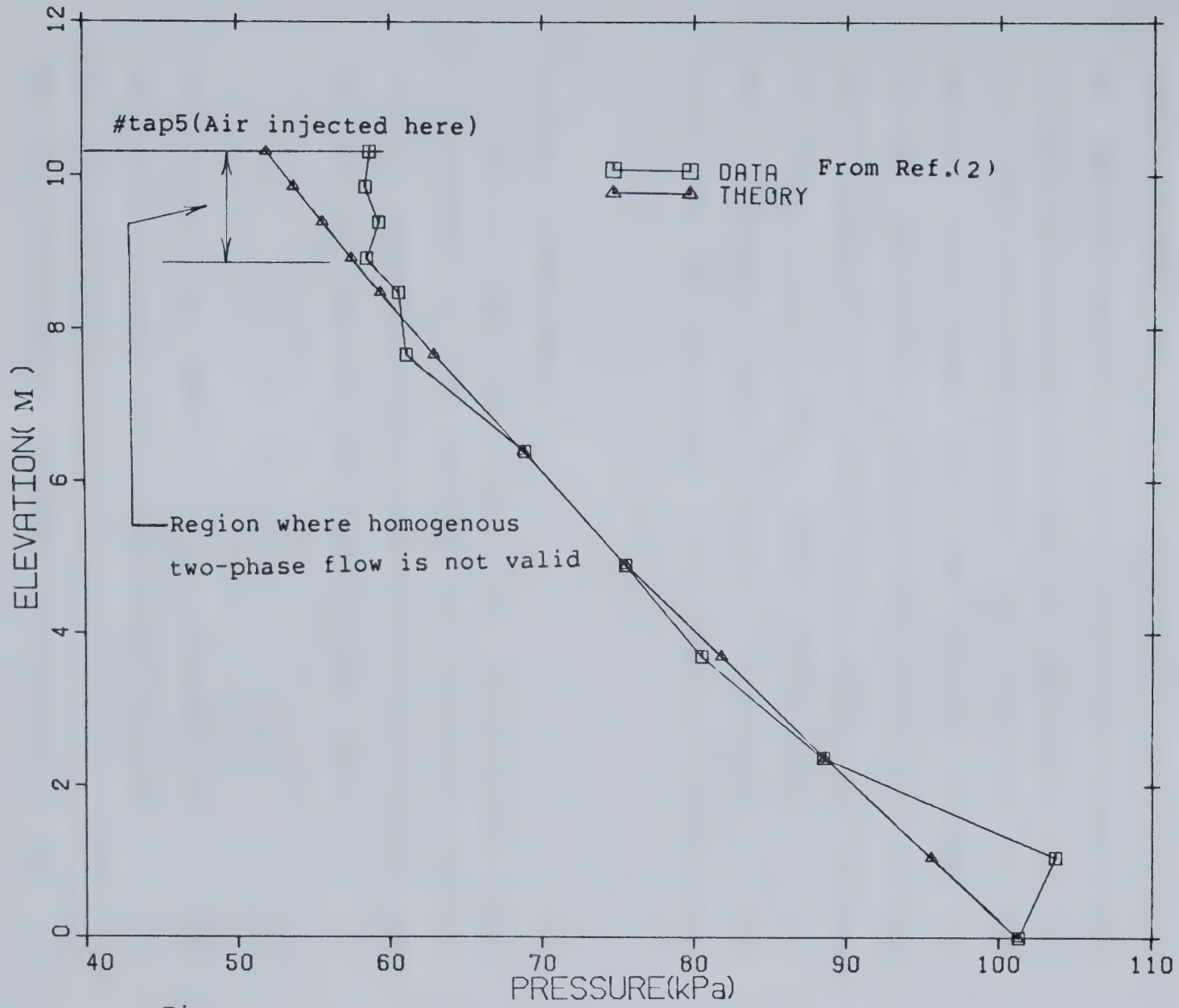

Figure 8 - Comparison between homogeneous two-phase flow theory and measurements of pressure changes in a vertical dropshaft

Nevertheless, this analysis may be applicable to cases where the drop shaft has been substantially undersized, or the discharge being substantially increased by relief sewers connected to the inlet. The head chamber is deep enough so that during heavy rain storm, the inlet becomes totally submerged and the drop pipe flows full. Moreover, the drop is so long that cavitation at the neck of the shafts becomes imminent. And suppose that some engineer realizes the situation and decides to construct air vents to relieve the negative pressure. Under these circumstances, the two-phase flow theory can be used to obtain adequate results. In any case, it is one of the many possible flow controls for drop shafts and its inclusion in the present discussion is necessary for a complete description.

2.3 Flow in Drop Shaft

If the flow does not fill the entire shaft cross-section, it is generally analysed by the Bernoulli criteria, assuming the flow remains coherent along the pipe wall, and the losses may be lumped into H_{ns}. Hence,

$$\frac{V_m^2}{2g} + h - \Delta z = \frac{V_2^2}{2g} + H_{ns} \qquad (59)$$

where h is the length of the dropshaft, and V_2 is the velocity at the outlet of the dropshaft. Therefore, if the head losses in the dropshaft are estimated, the velocity in front of the impingement area may be computed.

2.4 Plunge Pool Hydraulics

The plunge pool should be designed to effect energy dissipation and deaeration of the falling nappe, so that the violent turbulence can be confined to the pool area. The discharge into the outlet should be quiescent, clear, with low air content, and at an acceptable velocity.

The pool may employ either one of the two energy dissipation mechanisms: 1) hydraulic jump; or 2) jet diffusion. The geometry of the pool will be distinctly different depending on the dissipation principle adopted.

2.4.1 Hydraulic Jump Basin

If the pool is designed as a hydraulic jump dissipator, it should be elongated with a raised roof similar to the pool geometry employed by the TARP project of Chicago. The geometry of the energy dissipator is shown in Fig. 9. Weir and baffles were not used in the basin because of the observed poor hydraulic performance in the model, and the possible maintenance problems which may arise after every severe flood. In Anderson and Dahlin(1975)'s study, the basin was found to be effective in releasing the entrained air. It also performed satisfactorily for several tailwater levels. However, at the design discharge with low tailwater, the flow in the outlet sewer was observed to be supercritical and the estimated outlet velocity was approximately 7 m/sec. This velocity is probably too high for debris-carrying wastewater. Therefore, a deep sunken

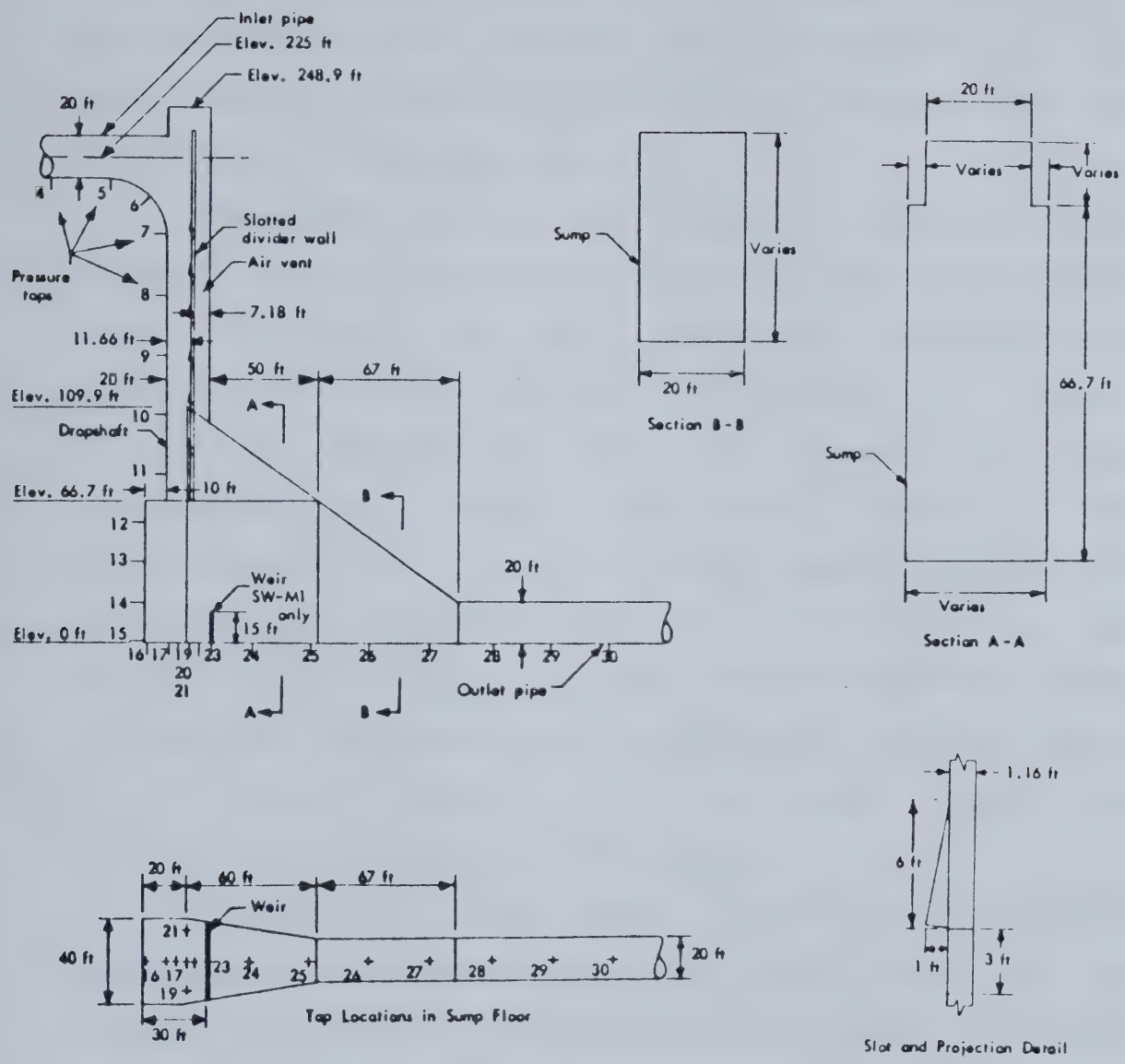

Figure 9 - Drop structure geometry adopted by TARP (From Anderson and Dahlin(1975))

basin may be needed for more effective energy dissipation at low tailwater depths. A forced jump is preferred to a free jump because the former requires a much shorter length and thus a lesser excavation volume.

A suggested pool geometry is shown in Fig. 10. As the downward flow strikes the plunge pool, it will be deflected into a backward flow and a forward flow if a backpool is provided. This has the desirable feature of strong circulation behind the flow which assists in energy dissipation. As a result, the kinetic energy of the supercritical flow in front of the jump may well be less than that predicted by the potential flow theory and the actual required basin length can be shortened. The benefit of providing the backpool and the potential for cost saving in a design situation will of course require the verification by a physical model study.

Upstream of the outlet sewer, a ground roller will form where debris will be trapped in circulation. This has the harmful potential of scouring the basin floor. A possible solution is to provide a sloping floor at the sewer entrance so that the basin will be self-cleaning and the erosion problem minimized.

Considering the control volume A in Fig. 8, the force balance in the horizontal direction may be written as:

$$F_f = F_3 + M_3 \tag{60}$$

where F_f is the back pressure force, F_3 is the total pressure at the y_3 section, and M_3 is the momentum flux

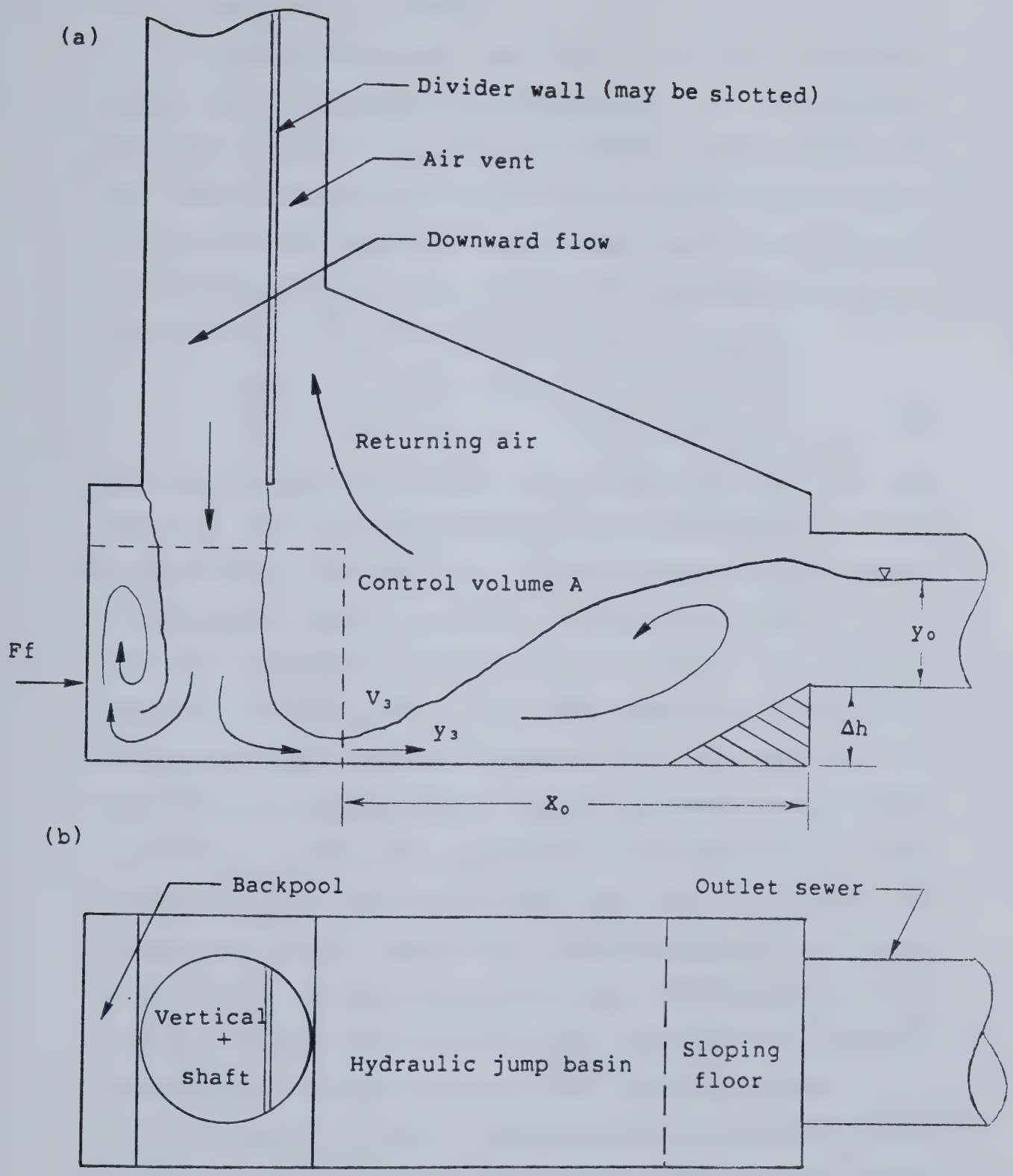

Figure 10 - A suggested geometry for the forced jump basin: (a)sectional view; (b) plan view

exiting the control volume A.

The forced hydraulic jump in a uniform rectangular sunken basin was analysed by Rajaratnam(1964). The effect of the step was accounted for by introducing a drag force, P_d, into the momentum equation. The drag force was defined as $[C_d \cdot (\rho V_3^2/2) \cdot \Delta h]$, where C_d is the drag coefficient, and Δh is the basin step height. With this, the momentum equation for the forced hydraulic jump may be written as,

$$\frac{\gamma y_3^2}{2} - P_d - \frac{\gamma y_o^2}{2} = \frac{\gamma q}{g} \cdot [\, V_{o,t} - V_3 \,] \qquad (61)$$

where y_3 is the supercritical flow depth in front of the jump, y_o is the flow depth in the outlet sewer, q is the discharge per unit width, $V_{o,t}$ is the outlet velocity, and V_3 is the supercritical velocity in front of the jump.

In Rajaratnam's experiments, at least six distinct forms of forced jumps could be observed by varying the distance of the step from the start of the jump, X_o. In order to minimize excavation volume, the basin length should be kept as short as possible. Nevertheless, energy dissipation and jump containment must remain effective. The values of C_d were determined experimentally for various X_o/L_{rj} ratios. A design chart was also developed so that for a given supercritical flow with the known tailwater level, a suitable basin length and step height may be chosen.

Presumably a similar procedure may be used to design the pool in Fig. 8. Some experimental observations will be needed to develop the design criteria and finalize the

appropriate pool geometry.

2.4.2 The Jet Diffusion Mechanism

If the pool is designed to effect energy dissipation by jet diffusion, it is recommended that its shape be circular. The shaft is preferably located directly above the center of the plunge pool so that the jet may expand in all directions. A sketch of the possible flow patterns in the pool is shown in Fig. 11. Due to the presence of the pool boundaries, the flow in the plunge pool may be divided into three regions: 1) the circular downward jet region; 2) the impingement region; and 3) the annular upward wall jet region. The extent of each of these regions will depend on the initial momentum of the jet , the jet size versus the plunge pool dimensions, air content, and pressure distribution in the pool.

The diffusion mechanism of a deeply submerged circular jet was discussed by Rajaratnam(1976). Since the jet belongs to the class of slender flows, it may require a pool depth of at least one order of magnitude larger than the jet size in order to achieve the required level of energy dissipation. As a result, it may not be economical to design an underground stilling pool utilizing the jet diffusion mechanism, unless some submergence exists in the plunge pool. Besides, debris is likely to be collected at the bottom of the plunge pool which will require routine dewatering and cleaning.

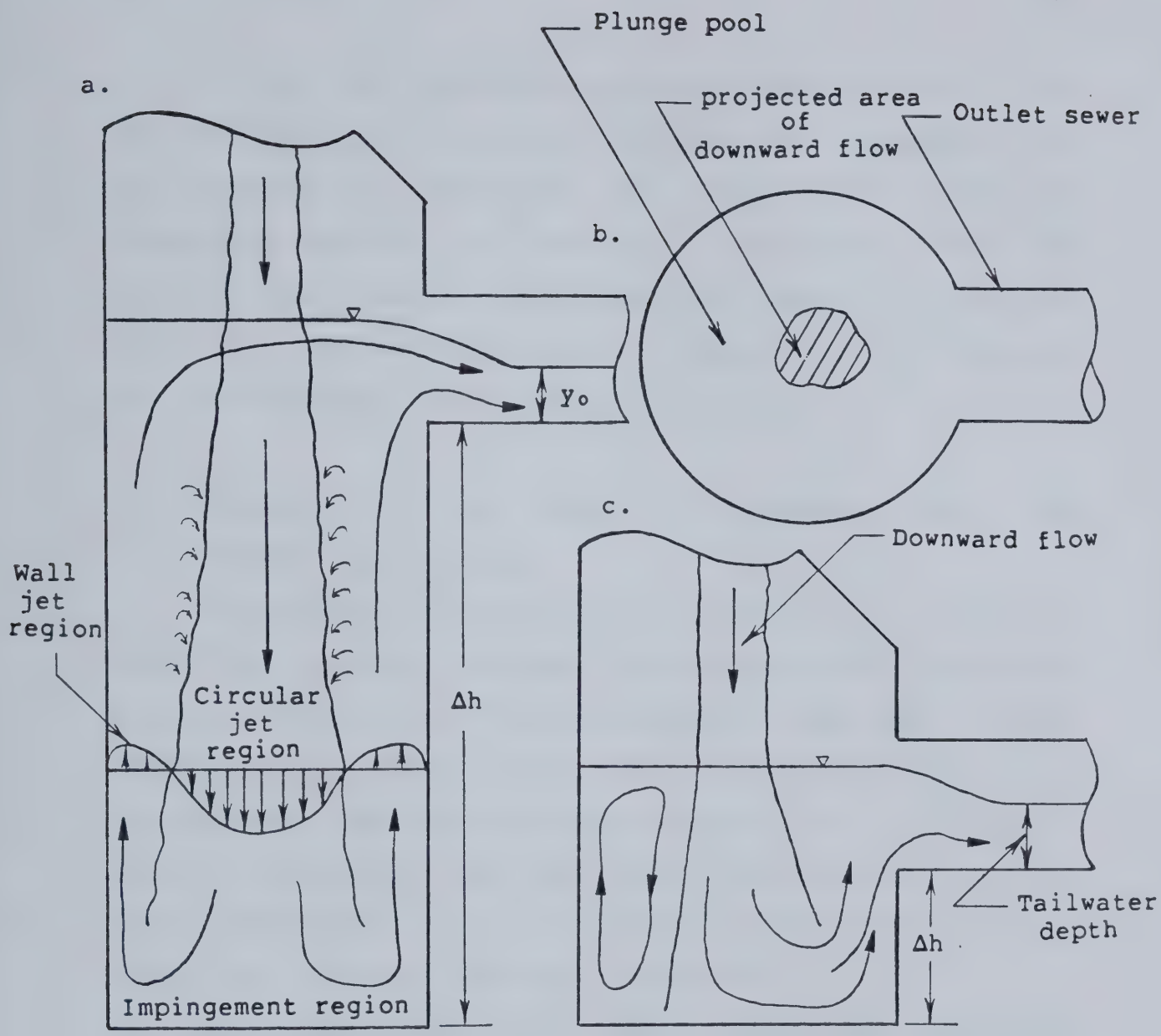

Figure 11 - Possible flow patterns in plunge pool:
a. when the pool depth is deep enough and the pool diameter large enough to effect energy dissipation
b. Plan view of plunge pool
c. when the pool depth is not deep enough to dissipate the kinetic energy of the flow, and the jet is deflected into the outlet sewer

Without any experimental observations, it is difficult to determine the most efficient plunge pool geometry. For the purpose of comparison, the plunge pool previously adopted by the City of Edmonton is evaluated using the forced jump criteria. This plunge pool geometry is shown in Fig. 12. A typical shaft size of fifteen feet is selected for the discussion in the following section.

2.4.3 Evaluation of the Plunge Pool Geometry Using the Forced-jump Criteria

To evaluate the adequacy of the plunge pool, a typical shaft drop structure is chosen for analysis using the forced jump criteria. Since the pool geometry has not been tested experimentally, there is no data available which would indicate the possible flow characteristics and the proper length requirements. In order to proceed with the analysis, it is assumed that the circular basin can be replaced by a square pool with the same major dimensions.

If a particular drop shaft has the following dimensions:

$$D = 15 \text{ ft.}$$

$$h = 100 \text{ ft.}$$

then, the plunge pool size is 1.5D or 22.5 ft., and the pool height, Δh, is 8.22 ft.. If the inlet sewer is horizontal and is designed to have a y_c/D value of 0.5 at the design discharge, using (14), the design discharge is computed to be 1485 cfs.

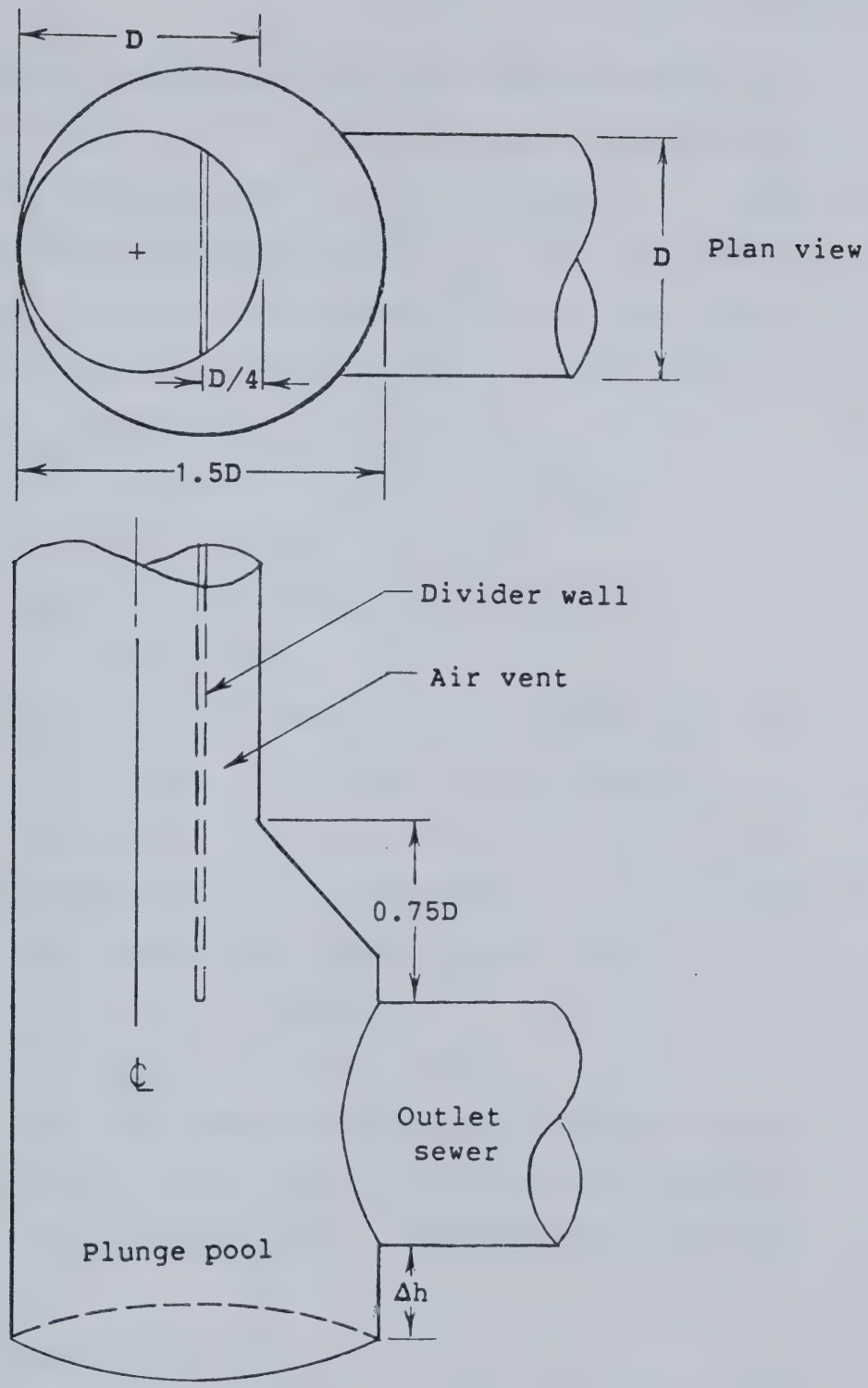

Figure 12 - Plunge pool geometry adopted by the City of Edmonton

A wide range of tailwater levels may exist depending on the downstream conditions. The most critical condition is probably when the outlet sewer is unsubmerged. In this situation the minimum tailwater depth, y_{o_t}, that would occur is probably equal to the critical depth. If both the inlet and the outlet are of the same size, this flow depth is equal to 7.5 ft. . From (26),

$$\Delta z = 11.51 \text{ ft.},$$

from (24), $V_m = 35.1$ ft./sec.,

and from (59), neglecting the losses in the shaft:

$$V_2 = 83.3 \text{ ft./sec.}$$

Now, if the velocity in front of the jump, V_3, is assumed to be the same as V_2, and the pool width, B, is equal to 1.5D, the average flow depth in front of the jump is 0.81 ft., the supercritical Froude number, F_3, is 16, and the sequent flow depth, y_2, which would exist in a horizontal basin is 17.9 ft. . Hence,

$$\psi_a = y_o/y_2 = 7.5/17.9 = 0.42$$

The distance from the step to the toe of the forced jump, X_o, is approximately 0.75D. The length of the surface roller, L_{rj} , is approximately 4.5 times the sequent flow depth. Hence,

$$X_o/L_{rj} = 0.14$$

From Fig. 13, C_d is 0.65 and the jump is within the type IV region but rather close to the type VI region. Type VI jump is not acceptable because the supercritical flow simply shoots over the step to form a swell behind the

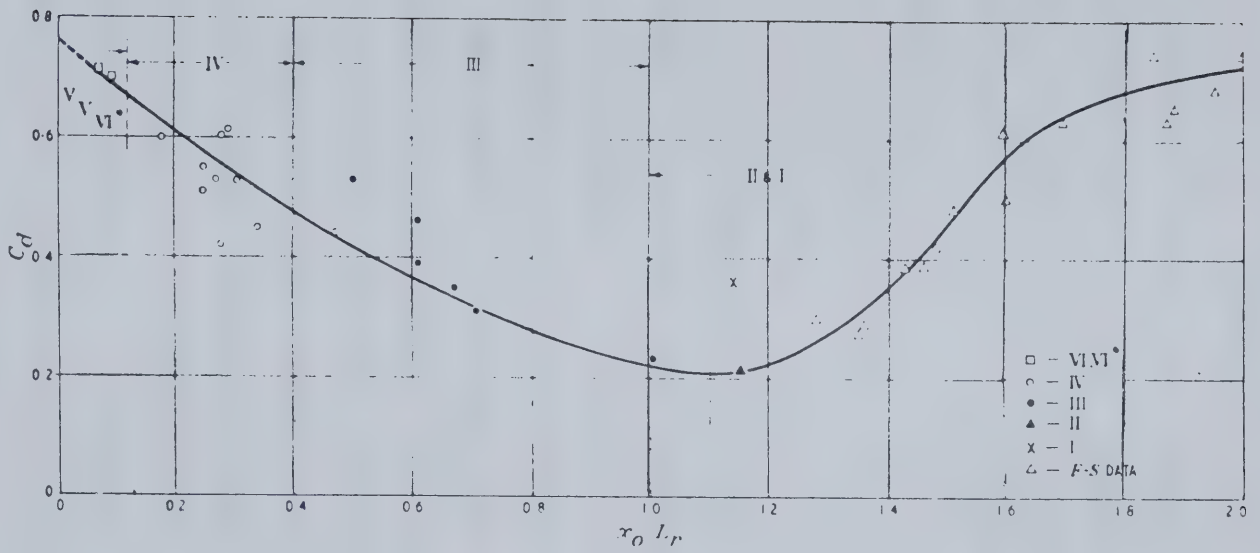

Figure 13 - Drag coefficient for a rectangular sunken basin (Rajaratnam(1964))

basin. This indicates that the basin is probably too short. From Rajaratnam(1964),

$$\Lambda = \frac{(\phi\psi_a - 1)\cdot[2F_3^2 - \phi\psi_a(1 + \phi\psi_a)]}{F_3^2\phi\psi_a} \qquad (62)$$

where $\Lambda = \beta C_d$, $\phi = y_2/y_3$, $\psi_a = y_o/y_2$, $\beta = \Delta h/y_3$, C_d is the drag coefficient due to the basin step, y_2 is the subscritical sequent depth, y_3 is the supercritical flow depth in the basin, and y_o is the outlet depth. For the present drop shaft,

$$\Lambda = \beta C_d = 1.45$$

Hence, $\beta = \Delta h/y_3 = 2.23$,

and $\Delta h(\text{required}) = 1.81$ ft.

Therefore, the Δh(provided) is approximately 4.5 times the required pool depth. If the basin is sufficiently long, energy dissipation will remain effective with a submerged hydraulic jump formed in the basin. However, if the length of the basin is too short, the supercritical flow will simply be deflected to enter the outlet sewer. These possible flow patterns are shown in Fig. 14.

Rajaratnam(1964) suggested that for good hydraulic performance, a type II to type IV jump should be chosen. For the following discussion, a type III jump with a drag coefficient of 0.4 is selected. From Fig. 11,

$$X_o/L_{rj} = 0.53$$

Hence, $X_o = 42.8$ ft.

and the minimum pool diameter required is:

$$X_o + 0.75D = 54 \text{ ft.}$$

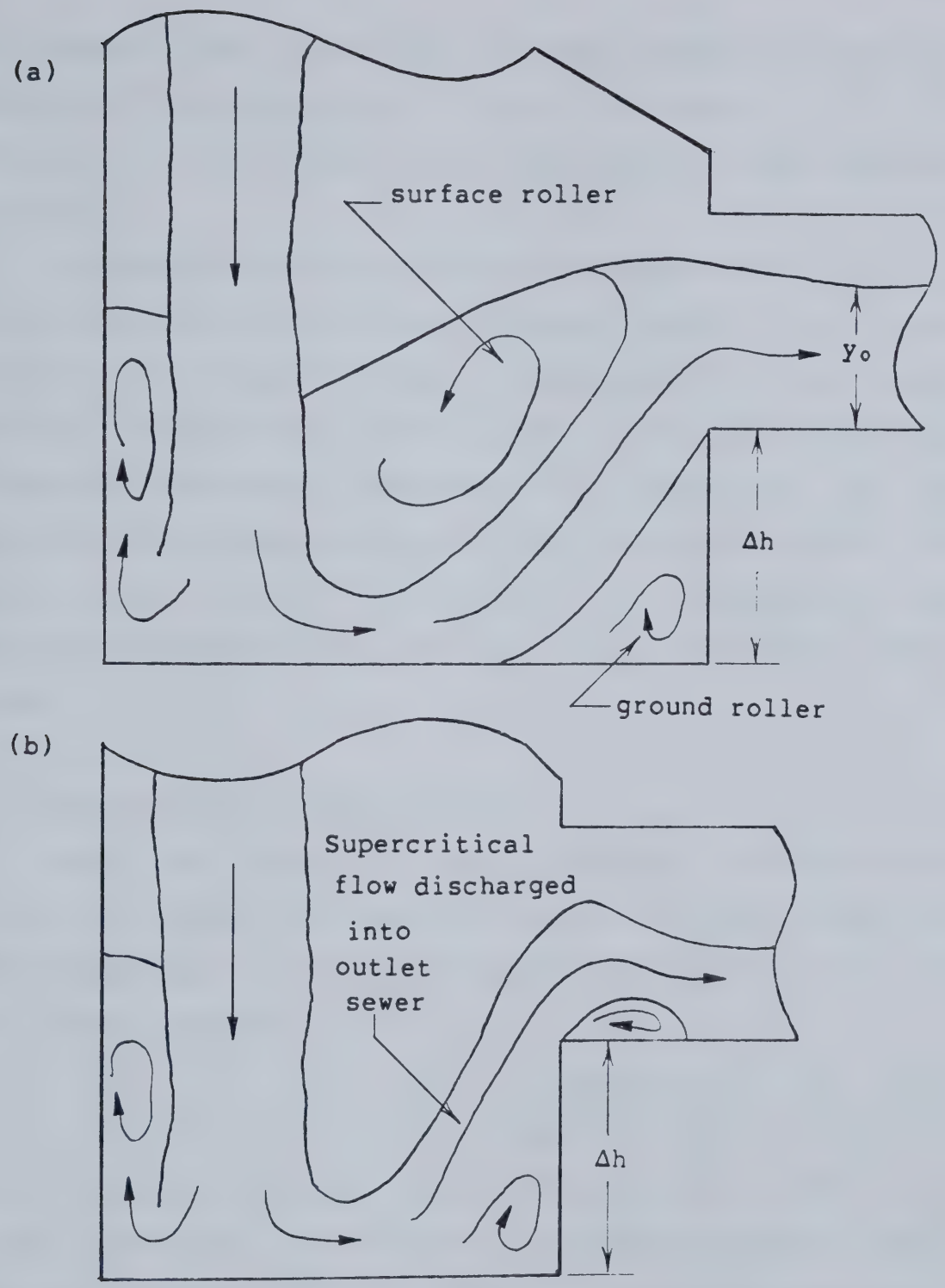

Figure 14 - Possible flow pattern in the hydraulic jump basin:
a. when the step is bigger than that required to form a forced jump but the length of the basin is long enough to contain the submerged jump;
b. when the step is deep and the length too short to form a jump, the supercritical flow is deflected into the outlet sewer.

A backpool may be provided if model studies indicate the benefits of incorporating it into the structure.
Since Λ is 1.451, and β is 3.63, the required step height is 2.9 feet.

The above calculation provides an approximate method of evaluation for the plunge pool geometry shown in Fig. 10. However, for future design, a model study is required to determine the adequate geometry and to verify the hydraulic concepts discussed. Hydraulics of plunge pool can be modelled fairly accurately using the Froudian criterion. In most cases, substantial reductions in construction and maintenance costs can be achieved by a laboratory model study.

2.5 Effect of Outlet Submergence

When the tailwater level increases above the sewer crown, the outlet sewer may flow full. In this situation, the water depth in the shaft may be determined by using the pipe-flow equation:

$$H_t = \left[K_e + K_o + f' \frac{L}{D} + f_v' \frac{H_v}{D_v} \cdot \left[\frac{A}{A_v} \right]^2 \right] \cdot \frac{V_d^2}{2g} \qquad (63)$$

where K_e is the entrance loss coefficient, K_o is the exit loss coefficient, f_v' is the Darcy-Weisbach friction factor for the dropshaft, L is the length of the outlet sewer, H_v is the submerged length of the dropshaft, D_v is the diameter of the dropshaft, A is the area of the outlet sewer, A_v is the area of the dropshaft, and V_d is the full flow velocity

of the outlet.

If the outlet conduit is horizontal, the depth in the vertical shaft, H_s, can be calculated as:

$$H_s = T_z + H_t - (V_v^2/2g) \quad (64)$$

or if the outlet conduit is at a slope S_o,

$$H_s = T_z + H_t - S_oL - (Q^2/2gA_v^2) \quad (65)$$

where T_z is the tailwater depth, and V_v is the average velocity in the drop shaft. A sketch of the submerged plunge pool is shown in Fig. 15. Submergence of the outlet will not alter the discharge capacity of the drop shaft unless the water level in the shaft rises to drown out the critical flow control section at the inlet.

2.6 Overloading

Since the discharge capacity is controlled by the terminal weir at the inlet, it will not be altered unless y_c/D becomes greater than 0.9 or the shaft entrance is flooded out. In the former case, the inlet conduit will flow full except near the outlet. The driving head is the head difference between the upstream manhole and the shaft entrance, minus the friction losses. The head discharge relation may be described by the full pipe-flow equation. In the latter case, the vertical shaft is completely filled. The discharge capacity may be determined by the full flow capacity of the outlet. The discharge in the inlet should be the same as that of the outlet under steady state conditions. If the inlet discharge thus computed is higher,

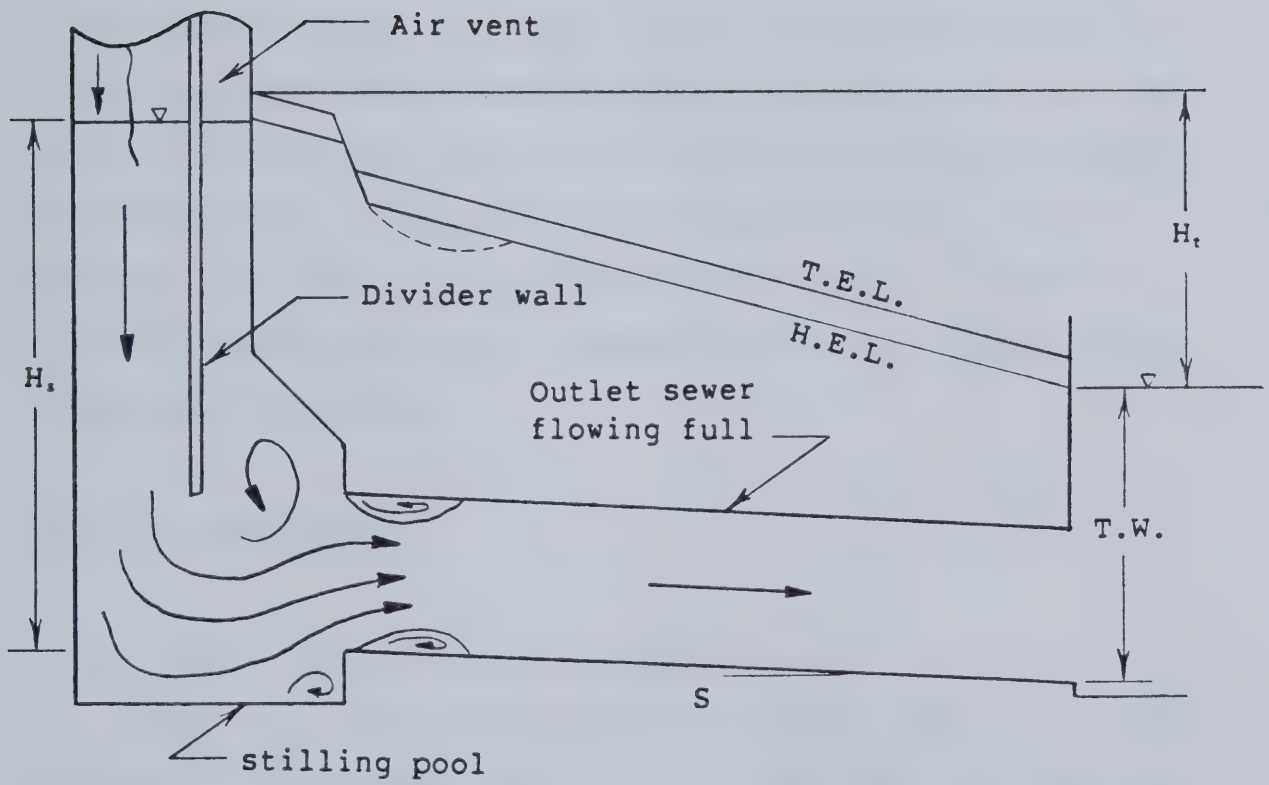

Figure 15 - Submerged plunge pool with outlet sewer flowing full

the water level in the shaft will rise to increase the discharge in the outlet. Otherwise, the water level will fall and the outlet discharge diminished.

2.7 Uplift Pressure

If the drop structure is situated below the groundwater-table, the pore water pressure at the base of the plunge pool may be sufficient to heave or crack it. The most critical condition occurs when the structure is empty. If field tests indicate that seepage forces will be a problem at the site, control measures such as providing a gravel blanket with drain pipes beneath the basin floor should be considered.

2.8 Air Entrainment

2.8.1 Types of Entrainment Processes

There are possibly four different kinds of air entraining processes which can be identified in a vertical drop shaft. These are: 1) the air entrainment due to the surface roller at the shaft entrance; 2) the free surface aeration of the flow in the shaft; 3) the forced aeration as the flow enters the water surface in the shaft; and 4) the air entrainment due to the hydraulic jump in the stilling pool at low tailwater. An assessment of these entrainment processes are as follows.

2.8.1.1 Surface Roller

When the shaft entrance does not have a smooth transition, the nappe will leave the inlet invert to impinge on the outer shaft wall. The flow will be deflected downward with a surface roller formed on top of the upper nappe causing local aeration. This aeration phenomenon was studied by Renner and had been summarized by Rao and Kobus(1975). Although the surface of impingement in Renner's study was not curved, the flow geometry is generally similar to the present case. In the absence of model studies, his results could be used for a rough estimate.

Some of the results in Renner's experiments are shown in Fig. 16. He showed that if the concentration of air in the deflected nappe beneath the surface roller is far from the state of saturation[2], the rate of air discharge to water discharge is proportional to the square of the jet's Froude number[3].

2.8.1.2 Surface Aeration in the Drop Shaft

As the flow runs down the shaft, its free surface will entrain air causing the flow to expand and become foamy. If the shaft is long enough, the jet may disintegrate into droplets and slugs of water. From limited experiments[4]

---

[2] The state of saturation corresponds to an air concentration, C, of about 0.4 to 0.5, or an air to water discharge ratio of about 0.7 to 1.0.

[3] For aeration to take place, the jet's Froude number must be greater than 1.

[4] The range of their experiments is:

$$0 \leq L_d < 3.0 \text{ m}$$

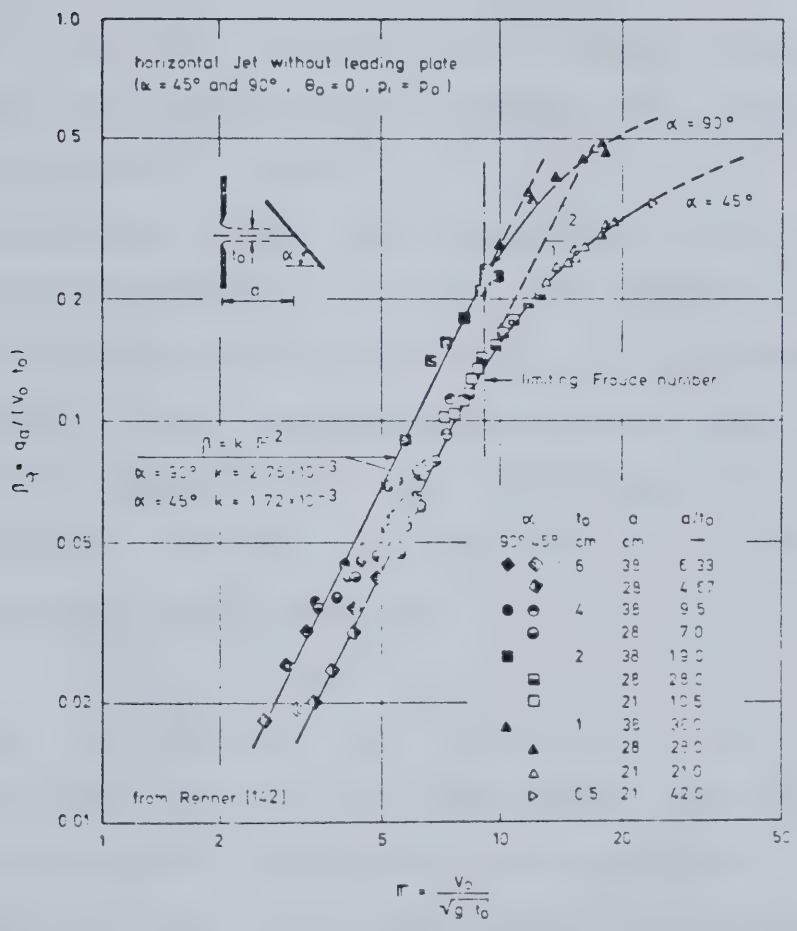

Figure 16 - Relative air entrainment in a horizontal jet (From Rao and Kobus(1975))

McKeogh and Elsaway (1980) established the following relationships for circular free waterfall:

For $\epsilon = 0.30\%$, $L_d = 66 \cdot Q_w^{0.42}$, (66)

for $\epsilon = 1\%$, $L_d = 38 \cdot Q_w^{0.369}$, (67)

and for $\epsilon = 5\%$, $L_d = 4.6 \cdot Q_w^{0.20}$, (68)

where L_d is the disintegration length, Q_w is the water discharge, ϵ is the turbulent intensity defined as $(\sqrt{\overline{u'^2}})/u_n$ and u_n is the jet velocity.

The process of free surface aeration in a rectangular flume was investigated by Straub and Anderson(1958). They studied the air concentration due to self-aeration in a rectangular flume with the slope ranging from 7.5° to 75°. From their experiments, they found that the mean air concentration in the fully-developed flow is a function of the slope and water discharge:

$$C_m = f_4(S/q^{1/5}) \quad (69)$$

where C_m is the mean air concentration of the fully developed flow, and S is the flume slope. However, it is not known whether their results can be extrapolated to represent the vertical flow in a drop shaft. It is likely that the process of aeration is similar in the early stage of the fall, with the characteristics deviating significantly as the jet begins to disintergrate. Again, further research is needed to clarify this.

---

[4](cont'd) $0 \leq Q_w < 1.1*10^{-3}$ m/sec.

Note that the disintegration length, L_d, is a strong function of the jet's turbulence level.

2.8.1.3 Forced Aeration by a Plunging Water Jet

The mechanisms of aeration when a high velocity flow enters a slower moving body of water was classified by McKeogh and Elsaway(1980) as: 1) annular oscillation; 2) intermittent vortex; 3) turbulent occlusion; and 4) droplet entrainment. Detailed descriptions of these mechanisms may be found in their paper.

As the water level in the shaft rises, the air transport capacity may vary. The rate of air transport will be governed by the entrainment capacity of the falling jet as well as the transport capacity of the flow below the water surface. Willock and Thorn(1973) identified three main regimes of air demand:

1. When the nominal fluid velocity is less than the threshold velocity for air flow, the entrained air will be retained in the zone of recirculation. Only very fine air bubbles can be discharged into the outlet tunnel below. Hence, the air demand is almost zero. This threshold velocity was determined to be about 0.13 m/sec. which is about one-half of the bubble rise velocity, for the range of bubble sizes between 1 mm and 5 mm in diameter.
2. In this case, the nominal fluid velocity remains less than the threshold velocity but the zone of recirculation is not completely contained within the shaft. As a result, some air is carried into the outlet tunnel. The length of the recirculation zone was found

to be about five to six times the shaft diameter and air transport will occur if the water column in the shaft is less than this value.

3. When the nominal shaft velocity is greater than 0.5 m/sec., which is about twice the bubble rise velocity[5], all the entrained air will be transported downward. The water level in the shaft will not change the air demand characteristics and the ratio of air to water discharge becomes a unique relation of the fall height. The air discharge is caused by a combination of self-aeration of the falling jet and the entrainment during impact with the water surface. The experimental results of the discharge ratio versus drop length is shown in Fig. 17.

In Thorn and Whillock's experiments, they found that the discharge ratio reaches a maximum at fall height of about 3.7 m. However, McKeogh and Elsaway(1980) found that the maximum volume of air entrainment is consistently about 10% higher than the volume at a fall height equal to the disintegration length. Since the disintegration length depends on the turbulence level and the fluid discharge of the flow, there is an apparent contradiction between the two investigations.

---

[5] The majority of air bubble sizes range between 1 to 5 mm in diameter. In this range, the air bubble rise velocity is about 0.26 m/sec. This size range has been found to be true for both models and prototype structures.

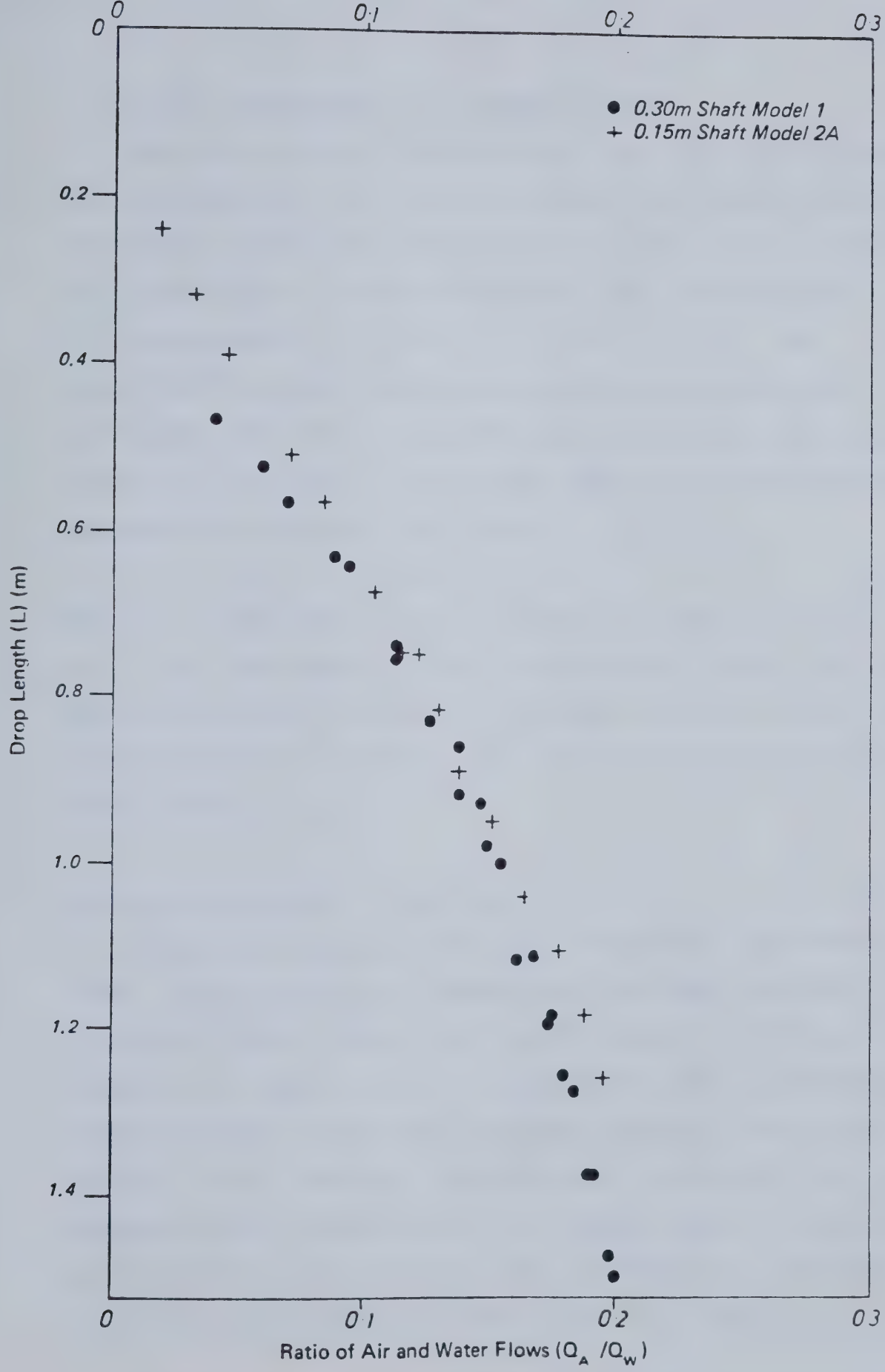

Figure 17 - Comparison of data from limiting air demand curves (From Whillock and Thorn(1973))

2.8.1.4 Air Entrainment by a Hydraulic Jump

When the tailwater level is low, the jet will strike the plunge pool at the bottom of the shaft where further entrainment takes place. If the pool is long enough to allow the formation of a stable hydraulic jump, the entrained air will be released by the surface roller. In this case, air demand will not be a problem as long as the plunge pool is ventilated. The rate of aeration by a rectangular hydraulic jump is a function of the Froude number which was shown by Kalinske and Robertson(1943) to be:

$$\beta = 0.0066 \cdot [\, F - 1 \,]^{1.4} \qquad (70)$$

where β is the ratio of air discharge to water discharge, and F is the supercritical Froude number. However, if the pool is too small to contain the jump and to allow the entrained air to escape, it will be discharged into the outlet tunnel.

2.8.2 Air Entrainment Modelling

Due to the complexity of the entrainment phenomenon, there is no satisfactory theoretical treatment available at this time. For the design of large hydraulic structures, models are usually made to investigate their operational characteristics and the various design options. Most dynamic aspects are modelled satisfactorily according to the Froudian criterion. However, such model studies tend to underestimate the rate of air entrainment. Kenn(1967) suggested that the inherent scale effect in predicting air

entrainment using the Froudian model may be due to surface tension and viscous effects. Ervine(1976), and McKeogh and Elsaway(1980), also added that in the case of air entrainment due to a water jet entering a pool of water, the turbulent intensity of the jet bears an important effect on the amount of air entrained.

Kenn(1967) proposed that if the model velocity and pressure force are of the same order of magnitude as that in the prototype, air entrainment may be satisfactorily modelled. Considering viscous and surface tension forces:

$$\frac{\text{Weber number}}{\text{Reynolds number}} = \frac{\rho V^2 l/\sigma}{\rho V l/\mu} = \frac{\mu V}{\sigma} \qquad (71)$$

which requires that $(\mu V/\sigma)$ is the same in both the model and the prototype structure. Using the same fluid in the model as in the prototype requires that V(model) be the same as V(prototype).

In Ervine's(1976) study, he found that for a jet striking an ambient water body, the ratio of air to water discharge is given by:

$$\frac{Q_a}{Q_w} = 0.26K\left[\frac{b}{P}\right]\cdot\left[\frac{H}{d}\right]^{0.446}\left[1 - \frac{V_o}{V}\right] \qquad (72)$$

where K is the proportion of the nappe perimeter exposed to the atmosphere, b is the nappe width, d is the nappe thickness, V is the velocity of the nappe, V_o is the incipient entrainment velocity, H is the height of fall, and P is the nappe perimeter.

The equation also indicates that air entrainment cannot be modelled by the Froudian criterion but requires that (V_o/V) be the same in both the prototype and the model. As indicated by Ervine, the incipient entrainment velocity is approximately the same for various jet sizes. In order to maintain similarity between the model and the prototype, the nappe velocity must be kept the same, or else the (V_o/V) ratio must be very small compared to one. Whillock and Thorn(1973) also concluded from their experimental studies that a distorted model with increased drop length, to allow the downward flow to attain prototype velocity, may provide a reasonable prediction of air demand.

The knowledge of air entrainment in a drop shaft is necessary in the design of the ventilation system. Previous experiences have shown that serious operational difficulties and a loss of service may result if air entrainment is not accounted for properly. Unless extensive experimental work is to be performed, the air demand of such structures may best be estimated from field measurements.

2.9 Modifications

Based on the above discussion, the following modifications may improve the efficiency of the shaft drop structures:

2.9.1 Inlet Transition

The entrance to the drop shaft should be smoothly curved. The flow cannot change its direction instantly and the presence of abrupt directional changes will cause the nappe to leave the lower boundary. The formation of a surface roller by the flow impinging on the pipe wall was discussed in an earlier section. This is undesirable because of the enhancement of turbulence and the reduction of the dropshaft capacity.

Flow around a vertical elbow may be roughly explained as follows:

Referring to Fig. 18 and assuming irrotational flow,

$$K = vr = v_o \cdot [r_o + y_e] = v_i r_o \tag{73}$$

and

$$Q = \int_{r_o}^{r_o+y_e} (vB)dr \tag{74}$$

where

$$B = D\sin\theta, \tag{75}$$

and

$$dr = 0.5D\sin\theta d\theta \tag{76}$$

Subsitute (73) into (74), we have:

$$Q = \int_0^{\cos^{-1}(1-2y_e/D)} \left[\frac{K/2}{r_o + D(1-\cos\theta)/2}\right] D^2\sin^2\theta \, d\theta \tag{77}$$

For a given discharge and curve radius, K can be solved for by using (77) and the velocity at any depth computed. Due to the increase in velocity near the boundary, the pressure may approach a cavitating level at high discharges. Therefore, the inlet transition curve should be smooth with

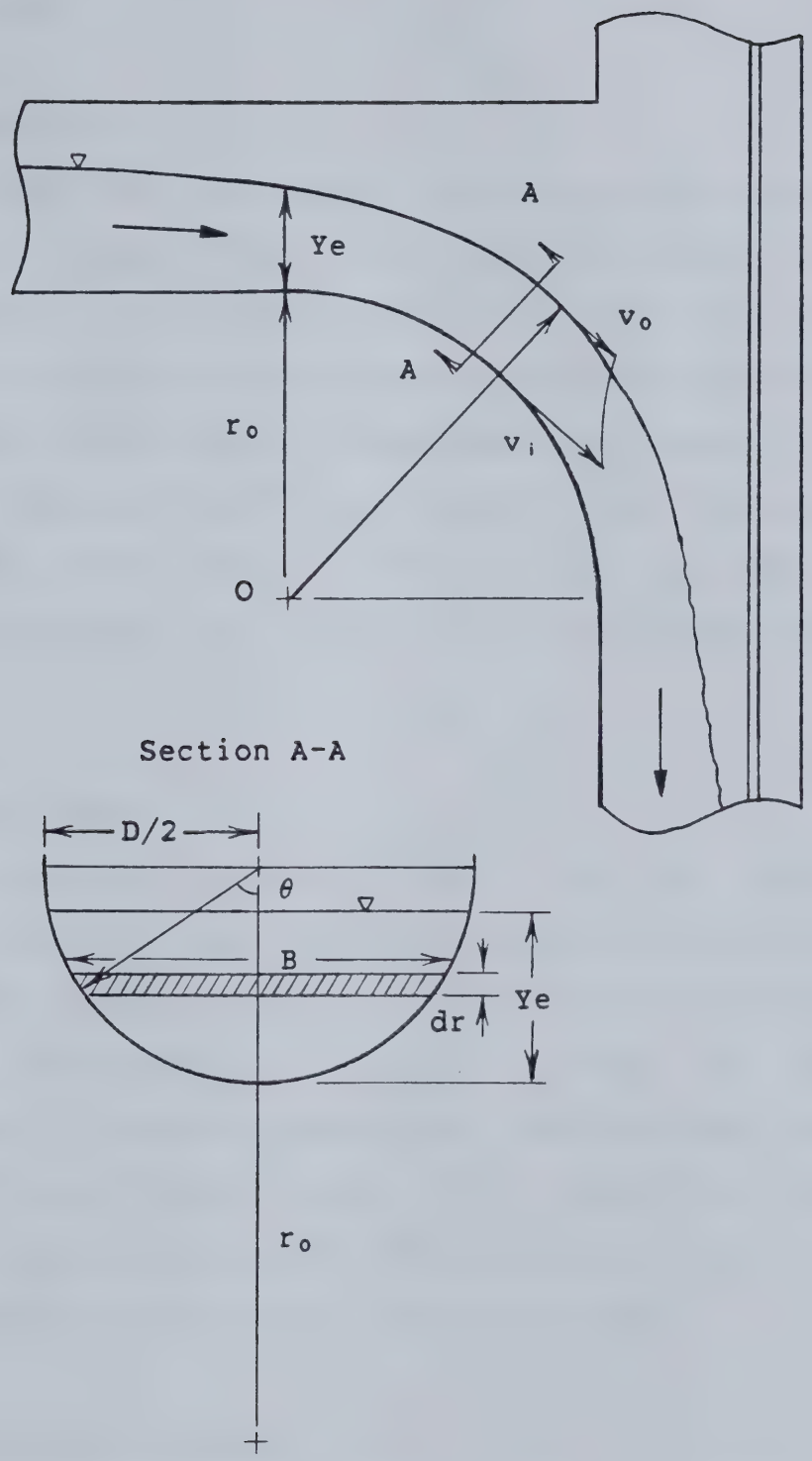

Figure 18 - Smooth inlet transition

a gradual directional change, or else the lower nappe should be ventilated.

2.9.2 Shaft Size

The drop shaft size should be at least the same as the inlet sewer size. Since there is no accurate way of predicting the air discharge, the higher shaft capacity can be used as a safety factor against unforseen conditions. In Anderson and Dahlin(1975)'s experiment, performance of the drop shaft does not seem to be impeded by the insertion of a divider wall other than a mild increase in the impact pressure measured in the plunge pool directly below the drop shaft.

2.9.3 Divider Wall

The partition wall for the inlet air vent should be slotted to provide continual aeration of the downward flow. As the flow accelerates down the shaft, its air demand will increase continuously. If air passage is impeded, subatmospheric pressure may develop. This suction head can cause a violent insufflation of air through the entrance. Besides, local pressures may reach the cavitational level causing excessive erosion to the pipe surface.

2.9.4 Plunge Pool Sizing

The possible modes of energy dissipation mechanisms and the appropriate plunge pool geometries were discussed

previously. Generally, it is desirable to have an elevated roof in the pool to allow the passage of returning air into the inlet air vent. A longitudinal pool is preferred over a circular pool in the TARP experience, which is also equipped with an inclined roof to provide ample clearance for air discharge. Venting the discharged air through the inlet will have the advantage of recirculating the air in the system and hence reducing the air demand from the inlet chamber.

If the pool is not long enough to contain a well formed jump, the supercritical flow may discharge into the outlet tunnel. This not only causes excessive erosion problems in the basin and the outlet sewer, but also allows the entrained air to be discharged into the outlet. In this situation, a downstream air-vent will be needed to prevent the formation of high pressure air pockets along the roof of the outlet. These air pockets may blow back through the entrance and set up unsteady surges in the shaft.

The optimal plunge pool geometry can best be determined from a model study. A forced jump basin with the features illustrated in Fig. 8 would probably be adequate for both energy dissipation and deaeration.

2.9.5 Outlet Sewer Sizing

From Anderson and Dahlin(1975), an outlet size equal to the inlet size is adequate to handle the design flood if the impact basin is well designed and ventilated. Indeed, if the outlet size is intentionally reduced, the flow depth at the

design discharge with no tailwater will be increased. Hence, the plunge pool depth may be proportionally reduced, resulting in a more economical basin design. However, when the tailwater level rises, and the shaft and the outlet conduit flow full, the energy losses from the entrance to the outlet may become critical. A smaller outlet size will have higher energy losses and a lower discharge capacity. In this situation, the entrance to the conduit may be bevelled to improve performance and to reduce head loss. In order to achieve optimal sizing of the outlet conduit, the range of operating tailwater must be known, and the plunge pool must be sized to effect energy dissipation and flow deaeration.

2.10 Recommendations

Based on the previous discussion, the following points can be suggested for the design of shaft drop structures:

1. The flow characteristics in a smooth entrance is superior to an entrance with abrupt changes. Various entrance configuratons should be tested by a model study to obtain an optimal design between economy and efficiency.
2. As discussed earlier, the flow conditions in the drop shaft can be very complicated and are heavily dependent on the entrance geometry. The actual flow configurations, be it a self-aerated open channel flow, or an air-controlled flow, and the possibility of local cavitation and separation in the shaft can best be

studied using a transparent model.

3. The theoretical derivations and assumptions presented should be verified by experiments before their application in future use.
4. A suggested plunge pool geometry is provided previously. The adequacy of the plunge pool should be tested with a model.
5. The outlet sewer does not need to be the same size as the drop shaft. The suitable size may be determined if the range of operating tailwater is known.
6. Extensive research has indicated that air entrainment cannot be modelled by the Froudian criterion. Some field measurements on the operating structures will be useful in sizing air vents which may be used to supplement experimental observations

3. Drill Drop Structures

3.1 Hydraulics

The hydraulics of the drill drop structures will be discussed in two parts: 1) the inlet sewer capacity; and 2) the drop pipe capacity. The efficient operation and structural economy will depend on the balanced sizing of the two components.

3.1.1 Inlet Sewer Capacity

Inlet sizing has been discussed in chapter 2. Generally, the inlet should be designed to operate with free outlet condition. If the conduit slope is mild, its capacity may be determined from the terminal-weir-control equation.

3.1.2 Drop Shaft Design

To determine the required sizes of the drill drop pipe and the head chamber, the entrance capacity must be known. In other words, the head-discharge relation of the horizontal orifice has to be determined.

3.1.2.1 Previous Studies on Horizontal Circular Weirs

Extensive investigations have been done on the discharge characteristics of circular weirs. Discharge coefficients had been given by Wagner(1954), Camp and Howe(1939), and Gourley(1911) for various weir heights and diameters.

Binnie(1938) had made some careful observations on the flow over a re-entrant vertical tube. From his studies, he classified the flow over circular weir into four possible categories: 1) weir flow; 2) Borda full flow; 3) Borda free flow; and 4) full-pipe flow. A description of these is summarized in Appendix III.

Although there is an abundance of research on circular weir, research on weir with zero sill height, which is quite common in many smaller structures, seems to be lacking. In the following section, the discharge over circular weir with zero sill height is derived analytically and the result is verified by experiments in the laboratory.

3.1.2.2 Circular Weir with Zero Approach Height - Momentum Analysis

Referring to Fig. 19, the momentum equation between the critical section and the end-depth section may be written as:

$$P_c - 2P_s\sin(\theta/2) - K_1P_e = \rho Q(V_e - V_c) \qquad (78)$$

where P_c is the critical pressure at sector A-A, P_s is the side pressure force, K_1 is the pressure coefficient, P_e is the end depth pressure, V_c is the critical velocity, V_e is the end-depth velocity, and θ is one-half of the inscribed angle of sector A-A. In the equation,

$$P_c = \int_{-\theta/2}^{\theta/2} (p_c\cos\phi r_c d\phi)\cdot y_c \qquad (79)$$

where ϕ is a dummy variable,

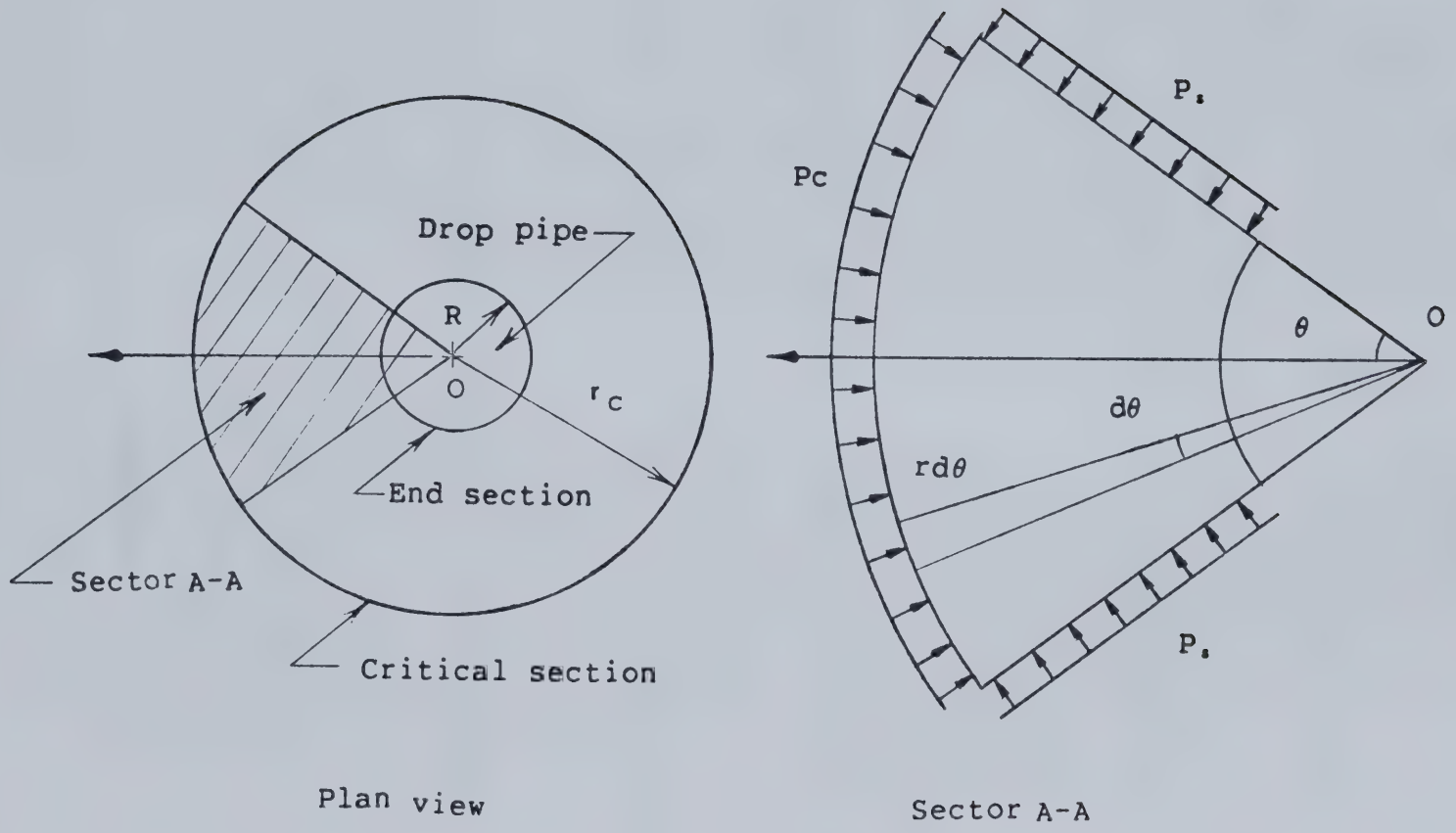

Figure 19 - Plan view of the head chamber floor

and $p_c = \gamma y_c/2$

Integrating with respect to the limits, we get:

$$P_c = \gamma y_c^2 r_c \sin(\theta/2) \tag{80}$$

and similarly, $$P_e = \gamma y_e^2 R \cdot \sin(\theta/2) \tag{81}$$

where r_c is the critical radius, and R is the radius of the drill drop pipe.

For an approach slope of zero, K_1 may be taken as zero. Therefore, the third term in (78) may be neglected. For the side pressure force:

$$P_s = \int_R^{r_c} \frac{\gamma y^2}{2}\, dr \tag{82}$$

If the water surface profile is approximated by a straight line, and for $R \le r \le r_c$,

$$y = y_e + (y_c - y_e)*(r-R)/(r_c-R) \tag{83}$$

Substituting $x = (r-R)/(r_c-R)$, $dr = (r_c-R)dx$, and (83) into (82),

$$P_s = \frac{\gamma}{2} \int_0^1 [y_e^2 + 2y_e(y_c-y_e)x + (y_c-y_e)^2 x^2](r_c-R)dx \tag{84}$$

Evaluating the above integral, we get:

$$P_s = (\gamma/6) \cdot (\, r_c - R \,) \cdot [\, y_c^2 + y_e y_c + y_e^2 \,] \tag{85}$$

If the discharge in sector AA is given by:

$$Q_\theta = \int_{-\theta/2}^{\theta/2} y_c V_c \cos\phi r_c \, d\phi \tag{86}$$

The critical velocity can be written as:

$$V_c = Q_\theta / [\, 2 r_c y_c \cdot \sin(\theta/2) \,] \tag{87}$$

Similarly, the velocity at the end section is:

$$V_e = Q_\theta/[\ 2Ry_e \cdot \sin(\theta/2)\ ] \tag{88}$$

Substituting (80), (81), (85), (87), and (88) into (78):

$$\gamma y_c^2 r_c \cdot \sin(\theta/2) - (\gamma/3)\cdot[r_c - R]\cdot[\ y_c^2 + y_e y_c + y_e^2\ ]\sin\theta = \rho Q_\theta^2\left[\frac{1}{2Ry_e\cdot\sin(\theta/2)} - \frac{1}{2r_c y_c\cdot\sin(\theta/2)}\right] \tag{89}$$

Equation 89 can be rearranged into:

$$2g\sin^2(\theta/2) - (2/3)g\sin^2(\theta/2)\cdot[1+y_e/y_c+(y_e/y_c)^2]\cdot(1-R/r_c) = Q_\theta^2/y_c^2 r_c\cdot[(1/Ry_e)-(1/r_c y_c)] \tag{90}$$

Now, if we substitute $\theta = 15°$, $\sin^2(\theta/2) = 0.067$, $Q = 12Q_\theta$, and $g = 9.81$ m/sec^2 into (90), and assume that $(r_c - R) \simeq 4y_e$, and $(y_e/y_c) \simeq 0.725$, we get:

$$Q = 12\cdot\sqrt{\frac{1.314y_e^3(R+4y_e)^2 - 3.944y_e^4(R+4y_e)}{0.5256\cdot(\ 0.275 + 4y_e/R\ )}} \tag{91}$$

Rearranging into a non-dimensional form:

$$Q^* = \sqrt{\frac{36.7(y_e/R)^3(1+4y_e/R)^2 - 101.2(y_e/R)^4(1+4y_e/R)}{(\ 0.275 + 4y_e/R\ )}} \tag{92}$$

where $Q^* = Q/g^{1/2}R^{5/2}$

Equation (92) gives the relationship between discharge and end depth for a circular weir with zero approach depth. Experiments were performed in the Graduate Hydraulic Laboratory to verify the above derivation. Details of the experiments will be discussed in a later section.

Let the head in the chamber be H:

$$H = y_e + (\ V_e^2/2g\ ) \tag{93}$$

Rearranging into a non-dimensional form:

$$\frac{H}{R} = \frac{y_e}{R} + \frac{1}{8\pi^2} \cdot Q^{*2} \cdot \frac{1}{(y_e/R)^2} \qquad (94)$$

Combining (92) and (94) will give a head-discharge relationship which is more convenient to use than (92) alone. This relationship is plotted in Fig. 20.

3.1.2.3 Full-pipe Flow and Cavitating Flow

As the head in the chamber increases, a point will be reached when the entrance water surface becomes level and the pipe begins to flow full. It is assumed that orifice control will not occur and the requirements of such is discussed in the next section. Then, depending on the length of the drop pipe to its diameter, cavitating flow may or may not occur.

The equation for the full-pipe flow is:

$$H + L_o = (1+f'L_o/D) \cdot (V^2/2g) + H_n \qquad (95)$$

where H is the head above the inlet entrance, H_n is the head loss at the entrance, and L_o is the length of the drill drop pipe. If the entrance loss is neglected, (95) may be rearranged into:

$$Q^* = \sqrt{\frac{2\pi^2 \left[\frac{H}{R} + \frac{L_o}{R} \right]}{\left[1 + f' \frac{L_o}{D} \right]}} \qquad (96)$$

The equation for cavitating flow is:

$$H - (P_c/\gamma) - H_n = (V^2/2g) \qquad (97)$$

where P_c is the cavitating pressure, and H_n is the lumped head loss. Equation 97 may be rewritten as:

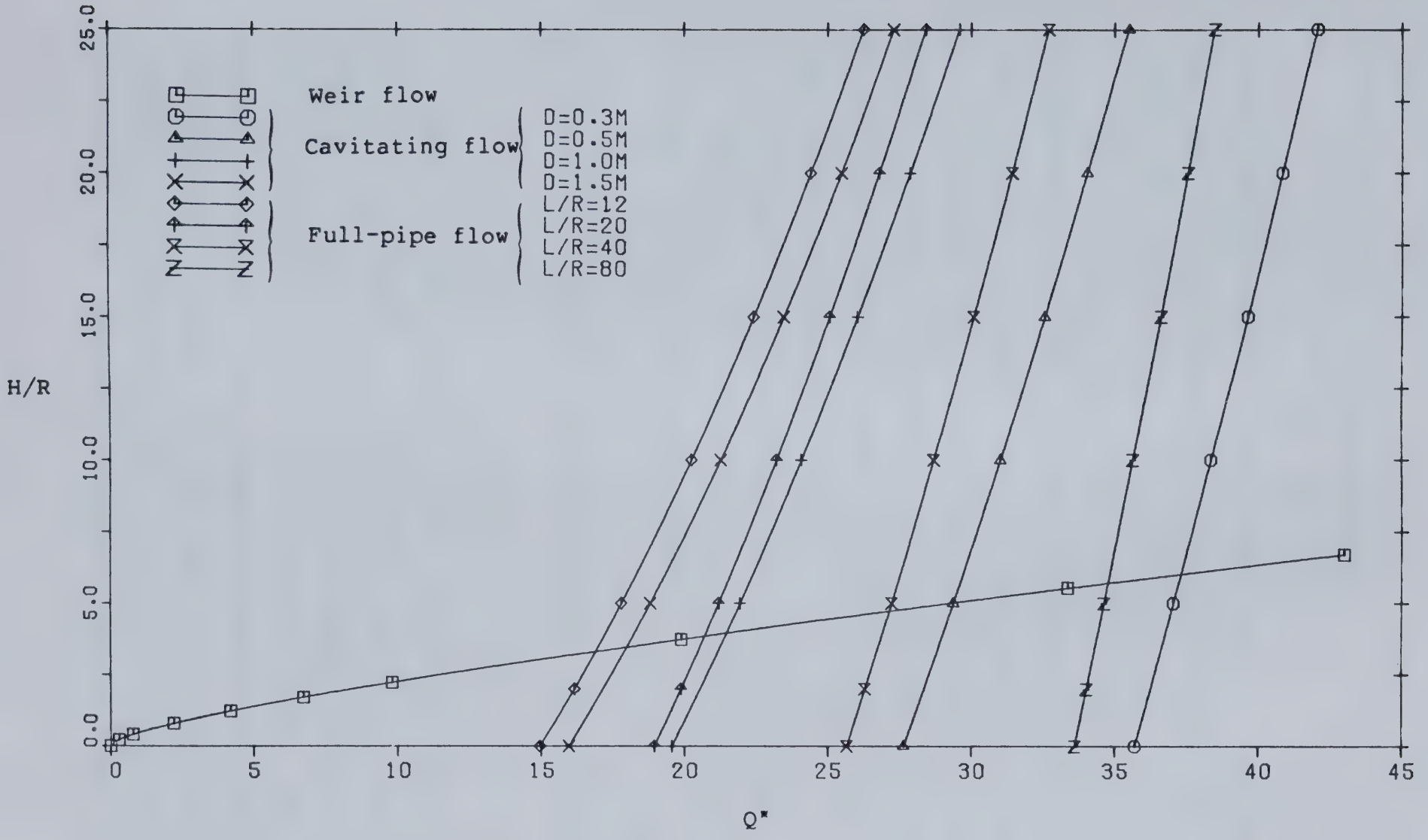

Figure 20 - Rating curves for a horizontal orifice

$$Q^* = \sqrt{2\pi^2\left[\frac{H}{R} - \frac{P_c}{\gamma R} - \frac{H_n}{R}\right]} \qquad (98)$$

For an open system with a head chamber above the drop shaft, and the entrance is designed so that orifice flow will not occur, three types of flow are possible: 1) the weir flow; 2) the cavitating flow; and 3) the full-pipe flow. Cavitating flow has been described by Anderson, Vaidyaraman, and Chu(1971). It occurs when the drop-pipe is long enough so that the pressure in the upper part of the conduit reaches cavitating pressure, P_c . This type of flow is particularly undesirable because cavitation will erode the shaft surface rapidly and severely.

Drop pipe can be designed so that cavitating flow will not control at any stage of discharges. From (47), the discharge for full-pipe flow is given by:

$$Q^* = f_6(H/R, L_o/R, H_n/R, f') \qquad (99)$$

and from (98), the discharge for cavitating flow is given by:

$$Q^* = f_7(H/R, D, H_n/R) \qquad (100)$$

Hence, if the roughness of the pipe and the loss at the entrance is estimated, cavitating flow can be avoided by choosing the length to diameter ratio properly. Equations 96 and 98 are plotted in Fig. 20 for several sizes and L_o/R ratios. The size of pipe should be chosen so that the weir flow curve will intersect the full-pipe flow curve before it intersects the cavitating flow curve. In any case, the drop pipe should be designed to operate within the weir flow

régime. Pipe flow would occur only in a state of surcharge.

3.1.3 Computer Program

The various flow controls discussed above are consolidated into a design program to facilitate the design of this structures. The program will evaluate, for a certain drop pipe size, drop height, and outlet water level, the head in the inlet chamber and the corresponding discharge. This is convenient for the evaluation of existing structures. In a design situation, the design discharge and drop height is known, the drop pipe size and the head in the inlet chamber are to be determined. In this case, one can determine the head capacity curves for a range of drop pipe sizes. The suitable drop pipe is the smallest size which passes the design discharge within the weir flow regime.

The program listing is included in Appendix III. Sample output is also included for a typical run. Due to the fact that head discharge relation deviate from the weir flow curve as the discharge increases, allowance should be provided to the head chamber depth so that surcharging will not occur prematurely. Besides, the program does not eliminate the need for a physical model study to verify the no-orifice flow assumption.

3.1.4 Methods to Prevent Orifice Flow

As presented earlier, orifice flow may be prevented by: 1) a smooth inlet transition; or 2) an enlarged entrance; or

3) the length to diameter ratio kept larger than 24.

1. The inlet may be designed to follow the lower nappe profile of circular overfall similar to that of a morning glory spillway. This entrance is efficient with little loss and no cavitation problems. For small structures, a less elaborate round entrance may be sufficient. Binnie(1938) was able to show that the use of a short rounded entrance was sufficient to suppress orifice flow.

2. The use of an enlarged sloping entrance as adapted by the City of Edmonton, may be effective in suppressing orifice flow. Due to the lack of experimental observation, we may assume that if the lower nappe is able to fill the pipe at a head equal to the head-chamber height, orifice flow will not occur. Some experimental nappe profiles over a sharp-crested circular weir are shown in Fig. 21. However, this inlet is not as efficient as the one described in (1) and it is not known whether cavitation will be a problem in the entrance.

3. Binnie(1938), in his experiments, demonstrated that for a sharp-crested, re-entrant tube having a length more than 24 times its diameter, orifice control may not govern, or that it may control the flow only momentarily before it changes back to full-pipe flow. This 'length to diameter' control seems to be a result of free surface entrainment in the pipe with the air

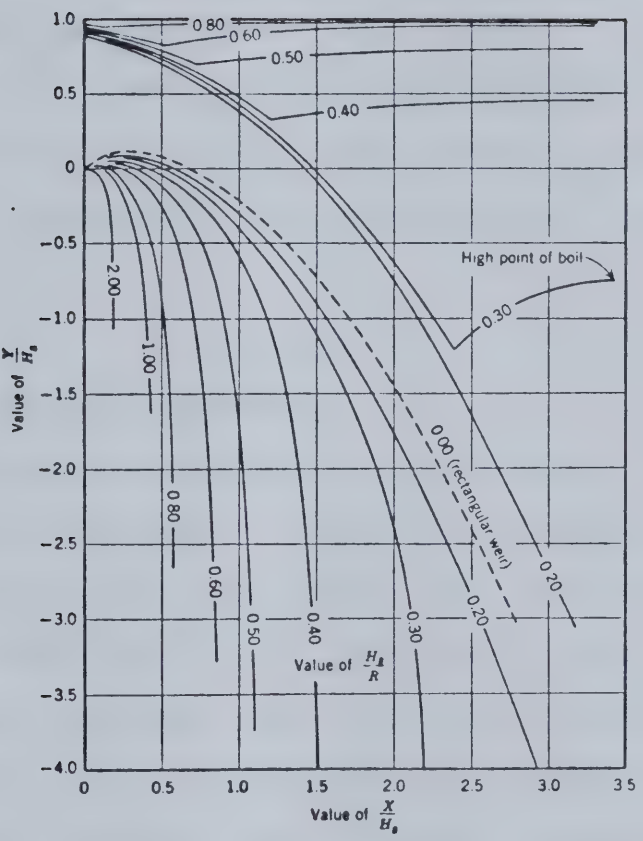

Figure 21 - Typical nappe surfaces for circular weirs (From Wagner(1956))

space being evacuated by the flow, hence prohibiting orifice flow formation. With zero sill height and an enlarged entrance, this required ratio could be much smaller.

3.2 Experiments on Horizontal Circular Weir

To verify the derivation of the weir flow equation (92) shown in section 3.1.2.2, an experimental investigation was carried out. Details of the apparatus and results are as follows.

3.2.1 Description of Apparatus

A sketch of the apparatus used is shown in Fig. 22. The tank A, in which the outlet pipe D was clamped, was square in plan, three feet by three feet, and three feet four inches in height. The outlet pipe with four inch inside diameter was four feet four and a half inches long made of plexiglass. It was inserted vertically through the bottom of the tank and clamped approximately at the middle of the pipe. A circular G.I. sheet of twenty-three inches in diameter was laid concentrically on top of the vertical pipe D, with a hole four inches in diameter at the center. Above the circular plate there were four rectangular plates held vertical by two blocks of wood which partitioned the upper chamber into four equal regions. The four vertical sheets in the upper chamber stabilized the approach flow and eliminated any vortexes so that the discharge over the tube

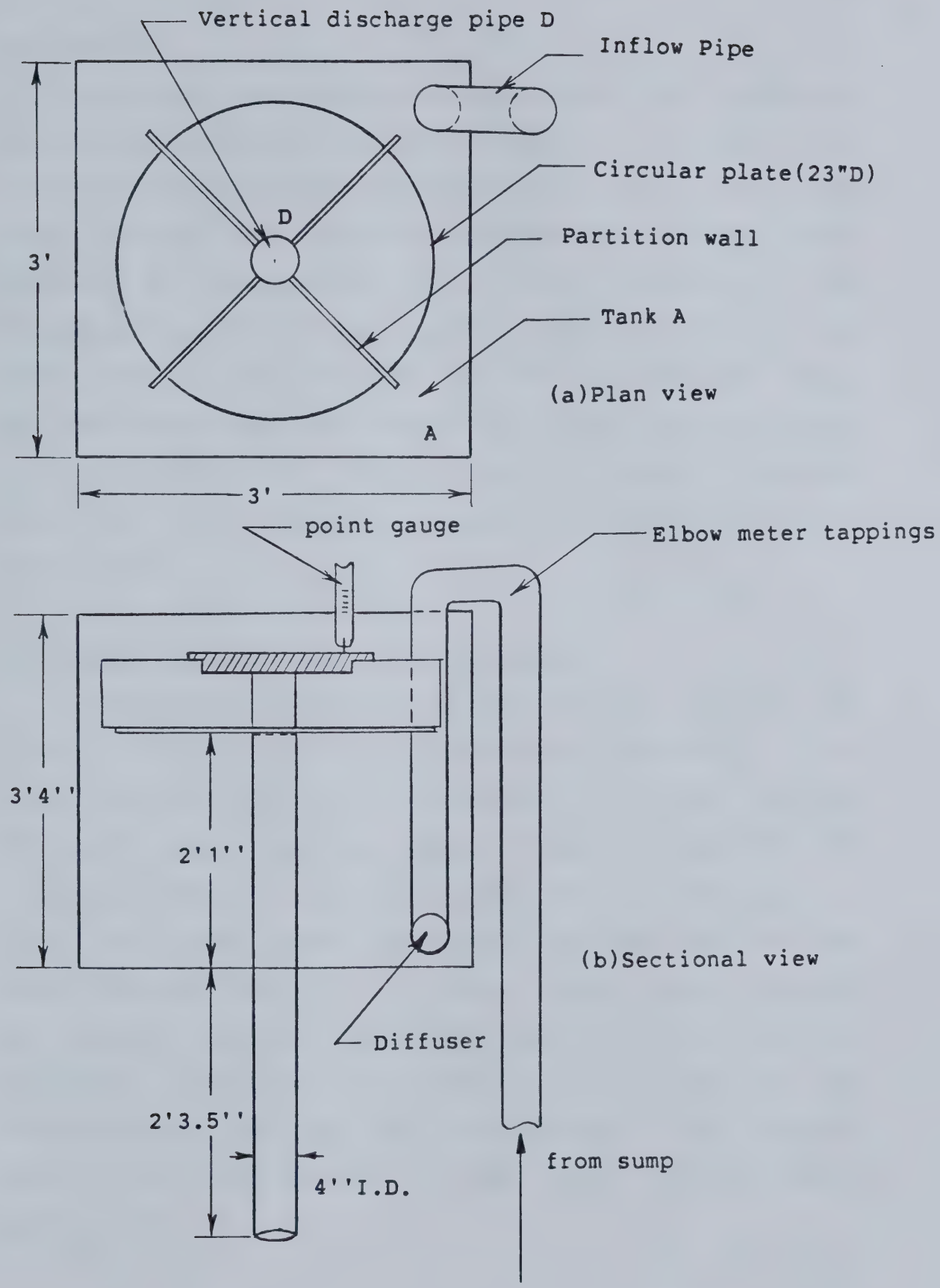

Figure 22 - A sketch of the circular weir apparatus

was radial.

The inflow was pumped from a sump below the apparatus to be discharged into the lower chamber of the tank A. The inflow line was equipped with a bypass to control the flow rate. The end of the inlet was mounted with a diffuser which assisted in suppressing vortexes and turbulence. The discharge from the vertical pipe D returned to the same sump where water was being pumped. The inflow was measured using an elbow meter which was calibrated in situ. The calibration curve is shown in Fig. 23. The depth of flow at various locations above the circular plate was measured using a point gage.

3.2.2 Experimental Observations and Data

As the head rose above the crest of the pipe D, the flow at first adhered to the vertical pipe wall. It was clear and quiet with no air entrainment. A further increase in head caused the lower nappe to leave the pipe wall and close the center of the pipe. At the center of the pipe, a boil was formed above the upper nappe. The flow remained clear and quiet near the crown of the pipe which expanded and turned white and foamy as it approached the outlet. An increase in discharge also caused the boil to rise. The top of the boil must be kept below the end depth of the circular weir if the theory derived in this report is to remain valid.

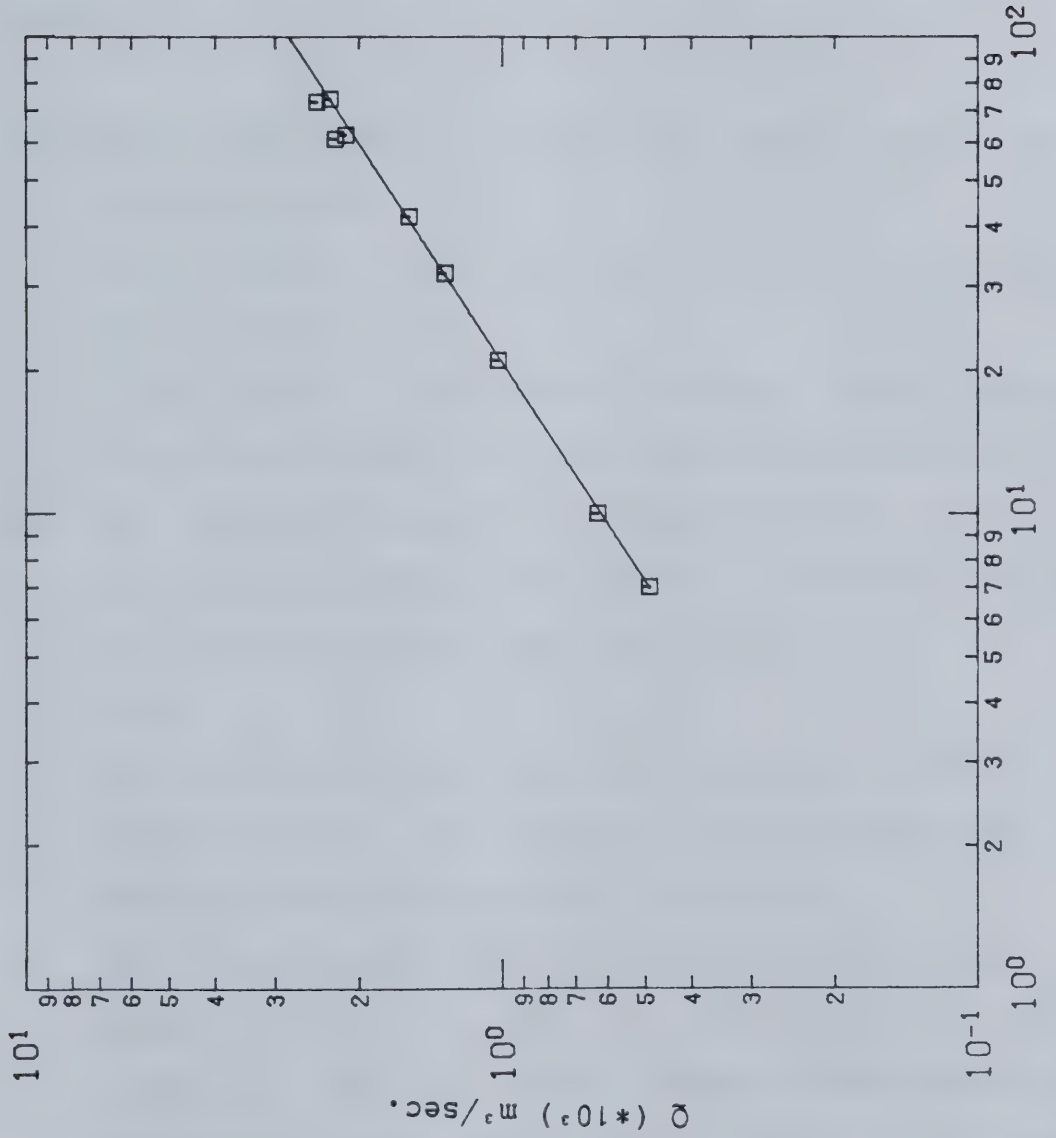

Figure 23 - Calibration curve for the elbow meter

Six sets of data were collected and tabulated in Table 2. The experimental results together with the theoretical weir flow equation were plotted in Fig. 24. If the boil rises above the critical depth of the approach channel, orifice flow will occur whose flow characteristics will be completely different from the weir flow discussed above.

3.3 Design and Balance Sizing of the Inlet Sewer and the Drill Drop Pipe

The criteria for sizing drill drop structures may be listed as follows:

1. Inlet size for the design discharge can be determined using the terminal-weir equation as discussed earlier.
2. The drop shaft should be designed in such a way that the design discharge will occur in the weir flow branch of the rating curve near the transition to full pipe flow.
3. The inlet entrance should be designed to avoid orifice control. Also, the length to diameter ratio must satisfy conditions to limit cavitation.
4. The head chamber depth should be at least equal to the head at design discharge, so that back-up will not occur at the inlet sewer. It may be desirable to keep the height larger than H as a safety factor against surcharge situation.
5. The head chamber should be provided with an antivortex

Table 2

Data and computation result for circular weir experiments

NO.	ye (m)	ye/R	Q^*	(m^3/s) Q(calc.)	(m^3/s) Q(measured)
1	0.0191	0.375	1.999	3.63×10^{-3}	3.55×10^{-3}
2	0.0157	0.309	1.490	2.71×10^{-3}	2.63×10^{-3}
3	0.0079	0.155	1.546	9.94×10^{-4}	1.00×10^{-3}
4	0.0100	0.197	1.766	1.39×10^{-3}	1.31×10^{-3}
5	0.0110	0.217	1.879	1.60×10^{-3}	1.57×10^{-3}
6	0.0130	0.256	1.124	2.05×10^{-3}	2.18×10^{-3}

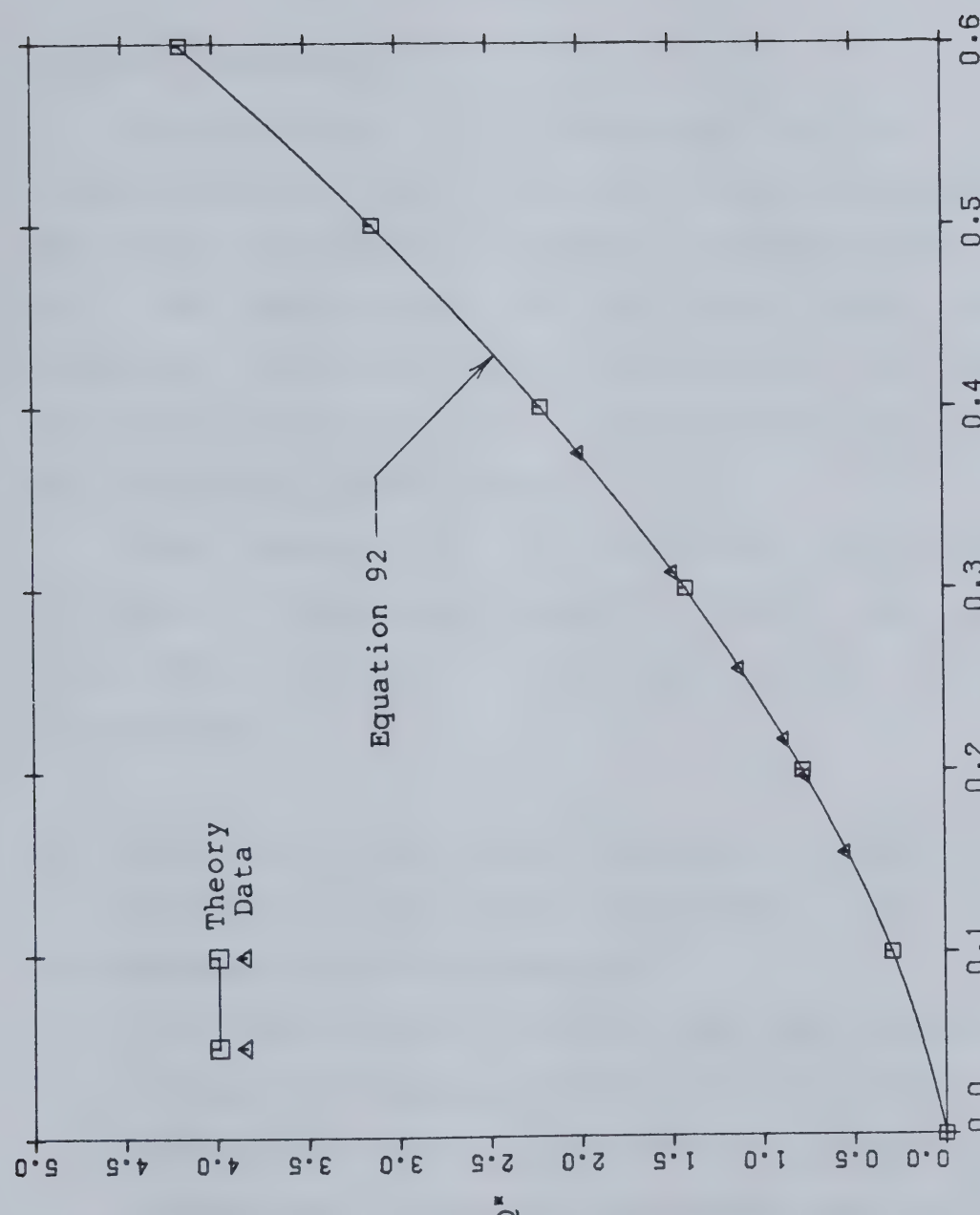

Figure 24 - Dimensionless rating curve for circular weir

device so that discharge through the drop pipe is not reduced by vortex formation. Two curtain walls across the diameter of the chamber will be sufficient to inhibit vortex formation.

3.4 Air Entrainment

Air entrainment of a circular wall jet in a vertical drop pipe penetrating a free water surface was summarized by Rao(1975) which seems to support a relation of the form $\beta = kF^2$. The experimental data is given in Fig. 25. In the relation, k was found to vary for different jet diameters. As explained in chapter 2, scale effect is inherent in most air entrainment model studies.

The discussion of air entrainment for the shaft drop structure is equally applicable to drill drop structure, with the exception of particulars due to geometric differences.

3.5 Modifications and Recommendations for Further Studies

Based on the above discussion, the following recommendations can be suggested:

1. Drop pipe entrance should be modified to avoid orifice control. Some approximate criteria to inhibit orifice control is given in section 3.1.4. Some experimental observations on the entrance geometry and the drop pipe sizing is needed to confirm satisfactory operation.
2. An anti-vortex wall should be provided to avoid vortex

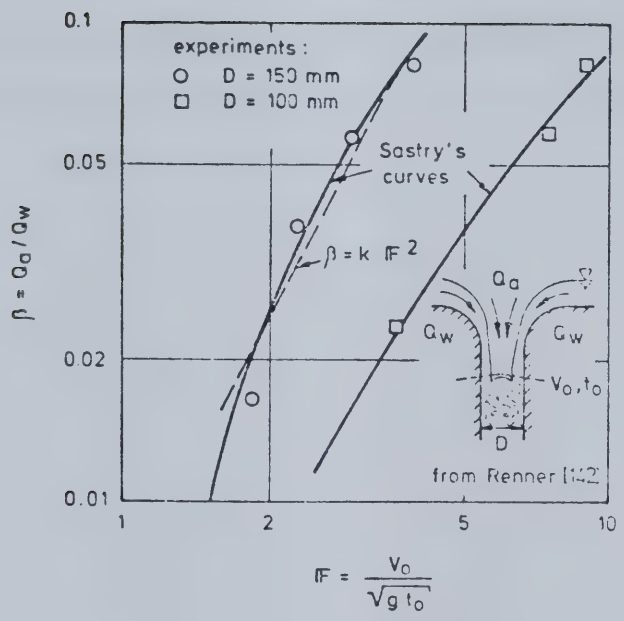

Figure 25 - Air entrainment in a ringshaped wall jet (From Rao and Kobus (1975))

formation in the chamber.

3. The entrance loss coefficient should be determined from experiments to facilitate designs.
4. The appropriate chamber size to drop pipe size should be determined to avoid boundary effects.
5. It was observed that the latter part of the weir flow curve changes into air-controlled flow. This type of flow is geometrically specific and requires a model study to accurately determine its rating curve.

4. Summary

The study evaluates the two types of drop structures used in the City of Edmonton.

For the shaft drop structures, the inlet capacity is evaluated using terminal weir equations for circular channel. The entrance condition to the shaft is important in determining the types of flow in the drop shaft, or whether cavitation is going to occur at the inlet, hence a smooth elbow is suggested in place of a 45° inclined floor.

The flow of air-water mixture is analysed and suggested as one of the possible flow types in the drop shafts. Aeration of flow is a major concern in the analysis of enclosed drop structures, since it is the most important element controlling the capacity of the structure. Some aspects of air entrainment has been discussed. The analysis of two-phase phenomenon dynamically is extremely complicated and difficult, even experimental approach have shown significant scale errors. Therefore, it is suggested that further work be done in this area.

The plunge pool is evaluated for effectiveness in the dissipation of kinetic energy before the flow entering the outlet. It is found that the plunge pool can be design as a hydraulic jump basin or a jet diffusion basin. Suggestions for the geometry of the basin is also included.

The effect of outlet submergence on the overall capacity of the structure, the problem with uplift pressure, overloading, balance sizing of various components are also

discussed.

For the drill drop structures, the circular weir flow equation is derived and verified with experiments. Weir flow is one of the flow types that can exist in these structures. The other possible types of flow are the full-pipe flow, the cavitating flow, and the orifice flow. Orifice flow can be avoided by providing a smooth inlet entrance. Cavitating flow can cause excessive wear to the pipe and should be avoided by proper design or by the provision of air vents.

The various types of flow controls, their governing equations, and the transitions from one type of flow to the next are summarized in a computer program. Discussion of air entrianment, balance sizing, and the control of orifice flow are also included.

Based on the results of the study, various modifications to the design of these structures have been suggested. Recommendations for further studies, especially the air entrianment aspects and the energy dissipations aspects of these structures, have been provided.

References

1. Anderson, A.G. and Dahlin, W.Q. **"Drop Shafts for the Tunnel and Reservoir Plan"**, St. Anthony Falls Hydraulic Laboratory project report no. 154, 1975
2. Anderson, A.G., Vaidyaraman, P.P., and Chu, C.S. **"Hydraulics of Long Vertical Conduits and Associated Cavitation"**, St. Anthony Falls Hydraulic Laboratory, U. of Minnesota, Minneapolis, project no. 11034 FLU, 1971
3. Binnie, A.M. **"The Use of a Vertical Pipe as an Overflow for a Large Tank"**, Proc. of the Royal Society of London, Ser. A., vol. 168, 1938, pp.219-237
4. Blaisdell, F.W. **"Hydraulics of Closed Conduit Spillways. Part I. Theory and its Application"** University of Minnesota, St. Anthony Falls Hydraulic Laboratory, Minneapolis, Technical paper no. 12, series B, 1952
5. Blaisdell, F.W. **"Hydraulics of Closed Conduit Spillways. Part II - Part VII, Result of Tests on Several Forms of the Spillway"**, University of Minnesota, St. Anthony Falls Hydraulic Laboratory, Minneapolis, Technical paper no.18, series B, 1958
6. Camp, C.S., and Howe, J.W. **"Tests of Circular Weirs"**, Civil Engineering, vol. 9, 1939, pp.247-248
7. Ervine, D.A. **"The Entrainment of Air in Water"**, Water Power & Dam Construction Journal, Dec. 1976, pp.27-30
8. Gourley, H.J.F., **"Experiments on the Flow of Water over Sharp-edged Circular Weir"**, Proceedings, Inst. of C.E.,

London, vol. CLXXXIV, 1911, pp.297-317

9. Henderson, F.M., **"Open Channel Flow"**, Macmillan Publishing Co., Inc., New York, 1966
10. Kalinski, A.A. and Robertson, J.M. **"Entrainment of Air in Flowing Water"**, Entrainment of air in flowing water -a symposium, Transactions, ASCE, vol. 108, 1943, paper no. 2205, pp.1393-1433
11. Kenn, M.J. **"Aspects of Similarity for Air-entraining Water Flows"**, Nature, Jan. 7, 1967, pp.59-60
12. McKeogh, E.J. and Elsaway, E.M. **"Air Retained in Pool by Plunging Water Jet"**, ASCE proceedings. J. of Hyd. Div., vol 106, HY10, Oct. 1980, pp.1577-1593
13. Moore, W.L., **"Energy Loss at the Base of a Free Overfall"**, Transactions, ASCE paper no.2204, Nov. 1941, pp.1343-1392
14. Rajaratnam, N. and Muralidhar, D., **"End Depth for Circular Channels"**, Proceedings, ASCE, Journal of Hyd. Div., vol. 90, HY2, Mar. 1964, paper no. 3828, pp.99-119
15. Rajaratnam, N., **"Turbulent Jets"**, Elsevier Scientific Publishing Co., Amsterdam, 1976
16. Rajaratnam, N., **"The Forced Hydraulic Jump"**, Water Power, Jan. and Feb. 1964
17. Rao, N.S.L. and Kobus, H.E. **"Characteristic of Self-aerated Free-surface Flows"**, Water and Waste Water - current research and practice, Vol. 10, Erich Schmidt Verlag, Berlin

18. Straub, L.G. and Anderson, A.G., **"Experiments of Self-aerated Flow in Open Channels"**, Proceedings, ASCE, Journal of Hyd. Div., Vol. 84, HY7, Dec. 1958, paper no. 1890

19. Wagner, W.E. **"Determination of Pressure-controlled Profiles"**, Morning-glory shaft spillways - A symposium, Transactions, ASCE, 1956, paper no. 2802, pp.345-383

20. Wallis, G.B., **"One-dimensional Two-phase Flow"**, McGraw-Hill Book Company, New York, 1969

21. Whillock, A.F. and Thorn, M.F.C. **"Air Entrainment in Dropshafts"**, Construction Industry Research and Information Association, Technical note no. 48, April 1973

Appendix I

Dimensionless quantities for circular channels

$\frac{y}{D}$	ψ	P^*	$\frac{y}{D}$	ψ	P^*	$\frac{y}{D}$	ψ	P^*
0.01	0.0257	0.0000	0.34	0.2734	0.0332	0.67	0.5194	0.1644
0.02	0.0373	0.0000	0.35	0.2808	0.0356	0.68	0.5267	0.1700
0.03	0.0470	0.0001	0.36	0.2882	0.0381	0.69	0.5341	0.1758
0.04	0.0556	0.0002	0.37	0.2956	0.0407	0.70	0.5341	0.1816
0.05	0.0637	0.0003	0.38	0.3032	0.0434	0.71	0.5487	0.1875
0.06	0.0715	0.0005	0.39	0.3104	0.0462	0.72	0.5560	0.1935
0.07	0.0790	0.0007	0.40	0.3179	0.0491	0.73	0.5633	0.1996
0.08	0.0864	0.0010	0.41	0.3253	0.0520	0.74	0.5705	0.2058
0.09	0.0937	0.0013	0.42	0.3328	0.0551	0.75	0.5777	0.2121
0.10	0.1009	0.0017	0.43	0.3403	0.0583	0.76	0.5849	0.2185
0.11	0.1080	0.0021	0.44	0.3477	0.0616	0.77	0.5921	0.2249
0.12	0.1151	0.0026	0.45	0.3552	0.0650	0.78	0.5993	0.2314
0.13	0.1222	0.0032	0.46	0.3627	0.0684	0.79	0.6064	0.2380
0.14	0.1293	0.0038	0.47	0.3702	0.0720	0.80	0.6136	0.2447
0.15	0.1364	0.0045	0.48	0.3777	0.0757	0.81	0.6207	0.2515
0.16	0.1434	0.0053	0.49	0.3852	0.0795	0.82	0.6278	0.2447
0.17	0.1505	0.0061	0.50	0.3927	0.0833	0.83	0.6349	0.2447
0.18	0.1576	0.0070	0.51	0.4002	0.0873	0.84	0.6420	0.2447
0.19	0.1647	0.0080	0.52	0.4077	0.0914	0.85	0.6490	0.2447
0.20	0.1718	0.0091	0.53	0.4152	0.0956	0.86	0.6561	0.2447
0.21	0.1790	0.0103	0.54	0.4227	0.0998	0.87	0.6632	0.2447
0.22	0.1861	0.0115	0.55	0.4302	0.1042	0.88	0.6703	0.2447
0.23	0.1933	0.0128	0.56	0.4377	0.1087	0.89	0.6774	0.2447
0.24	0.2005	0.0143	0.57	0.4451	0.1133	0.90	0.6845	0.3158
0.25	0.2077	0.0157	0.58	0.4526	0.1179	0.91	0.6917	0.3233
0.26	0.2149	0.0173	0.59	0.4601	0.1227	0.92	0.6990	0.3308
0.27	0.2221	0.0190	0.60	0.4675	0.1276	0.93	0.7064	0.3384
0.28	0.2294	0.0207	0.61	0.4750	0.1326	0.94	0.7139	0.3460
0.29	0.2367	0.0226	0.62	0.4824	0.1376	0.95	0.7217	0.3537
0.30	0.2440	0.0255	0.63	0.4898	0.1428	0.96	0.7298	0.3615
0.31	0.2513	0.0266	0.64	0.4972	0.1481	0.97	0.7384	0.3692
0.32	0.2586	0.0287	0.65	0.5046	0.1534	0.98	0.7480	0.3770
0.33	0.2660	0.0309	0.66	0.5120	0.1589	0.99	0.7597	0.3848
						1.00	0.7854	0.3927

Appendix II - Binnie's Description of Flow over a Re-entrant Tube

Types of flow over a vertical re-entrant tube

Binnie(1938) investigated the types of flow over a two-feet-long tube with one inch inside diameter. The tube was clamped to the base of a large tank at the middle of the pipe. From his experiments, he identified the following possible flow types:

1. **Weir flow:** As the head rises above the crown of the tube, water flows down the surface forming an annular jet with a glassy appearance. As discharge increases, the flow becomes more violent, of the noisy "gulping" type, with air entrainment at the center of the tube. Intermittent vortex may also form. The functional relationship is generally written as $Q = f_s(H^{3/2})$.
2. **Borda free flow:** This is the same as orifice flow described in the main text of this report. This flow stage is quiescent with little air entrainment. The water surface in the tank is about level. As Binnie(1938) described, *"The issuing stream assumed the appearance of a thin fixed glass rod projecting from the center of the pipe but not touching"*.
3. **Borda full flow:** As the stage of the Borda free flow drops, the water surface above the tube suddenly opens up with the downward stream deflected to adhere to the tube surface. This is similar to the early stage of weir flow except for a small ring of air entrapped

around the inner surface of the top of the pipe.

4. **Full pipe flow:** This occurs when the head above the tube becomes very high. The tube flows full, quiet, with no air entrainment. This flow may exist at the same stage as the orifice flow and which governs will depend largely on the geometry of the tube inlet. Some methods of preventing orifice flow are discussed in the main text. The functional relation of this flow is generally written as $Q = f_9(H^{1/2})$.

Appendix III - Computer Program for the Design of Drill Drop Pipe and Sample Output

```
1     C  THIS PROGAM UTILIZES THE HYDRAULIC CONCEPTS PRESENTED
2     C  IN THE REPORT " A PRELIMINARY STUDY OF DROP STRUCTURES
3     C  IN THE EDMONTON STORM WATER SYSTEM " TO PROVIDE A TOOL
4     C  FOR THE ANALYSIS AND SIZING OF THE DRILL DROP STRUCTURES.
5     C
6     C
7     C  MAIN PROGRAM
8     C
9     C
10          COMMON DIAM, ENDPH(20), QDROP(20), AINIYE, GRAVTY, CHDIAM
11          COMMON /SUB02/ HWEIR(20), HFULL(20), HCAVI(20)
12          COMMON /SUB03/ALENGT,FPRIME, PRDOWN, ALOSSC(20),ALOSSB,PRCAV
13          COMMON /SUB04/ AMANN, IUNIT, QMAX, QMIN, ISTART
14    C
15    C
16    C  DIAM   = DIAMETER OF DROP PIPE
17    C  ENDPH  = END-DEPTHS
18    C  QDROP  = DISCHARGES
19    C  AINIYE = INITIAL VALUE OF END-DEPTH
20    C  GRAVTY = GRAVITATIONAL ACCELERATION
21    C  HWEIR  = HEAD FOR WEIR FLOW
22    C  HFULL  = HEAD FOR FULL-PIPE FLOW
23    C  HCAVI  = HEAD FOR CAVITATING FLOW
24    C  ALENGT = LENGTH OF DROP PIPE
25    C  FPRIME = FRICTION FACTOR OF PIPE
26    C  PRDOWN = PIEZOMETRIC PRESSURE HEAD AT OUTLET
27    C  ALOSSC = ENTRANCE LOSS OF DROP
28    C  ALOSSB = BEND LOSS OF DROP
29    C  PRCAV  = PRESSURE HEAD AT CAVITATING REGION
30    C  AMANN  = MANNINGS N
31    C  QMAX   = MAXIMUM DISCHARGE
32    C  QMIN   = MINIMUM DISCHARGE
33    C  IUNIT  = TYPE OF UNIT USED (BRITISH OR METRIC)
34    C  ISTART = FLAG INTICATING TERMINATION OR GOING AHEAD
35    C
36    C
37     1    CALL READ
38          IF (ISTART .GE. 1) GO TO 99
39          CALL DETRMN
40          CALL PREPAR
41          CALL PRINT
42          CALL ENDPTH
43          CALL HEAD
44          CALL RESULT
45          CALL PRINT2
46          GO TO 1
47     99   STOP
48          END
49    C  THIS SUBROUTINE WILL INTERPOLATE FOR THE CONTRACTION
50    C  COEFFICIENT (ALOSSC).
51    C
52    C
53    C
54          SUBROUTINE PREPAR
55          COMMON DIAM, ENDPH(20) , QDROP(20), AINIYE, GRAVTY, CHDIAM
56          COMMON /SUB03/ALENGT,FPRIME, PRDOWN, ALOSSC(20), ALOSSB, PRCAV
57          DIMENSION VEL(14), D2D1(14), TABLE(14,14)
58          DATA VEL/0.,.2,.3,.4,.5,.6,.7,.8,.10,.12,.15,.20,.30,.40./
59          DATA D2D1/1.0,1.1,1.2,1.4,1.6,1.8,2.0,2.2,2.5,3.0,4.0,5.0,
```

```
60          *10.0,99999./
61           PIE1 = 3.14159265
62             READ(3,501) ((TABLE(I,J),J=1,14),I=1,14)
63      501    FORMAT (7F4.2)
64           DO 550 K=1,20
65               VELCTY = QDROP(K)/PIE1/((DIAM/2.)**2)
66               IF (VELCTY.GE.40.) GO TO 561
67               KK = 1
68      502      IF ( VELCTY.LT.VEL(KK) ) GO TO 503
69               KK = KK+1
70               GO TO 502
71      503      R3LATE = VEL(KK)
72               R3ERLY = VEL(KK-1)
73               JJ = 1
74               RD2D1 = CHDIAM/DIAM
75      504      IF ( RD2D1.LT.D2D1(JJ)) GO TO 505
76               JJ = JJ+1
77               GO TO 504
78      505      R4LATE = D2D1(JJ)
79               R4ERLY = D2D1(JJ-1)
80               RANGE1 = TABLE(JJ-1,KK) - TABLE(JJ-1,KK-1)
81               RANGE2 = TABLE(JJ,KK) - TABLE(JJ,KK-1)
82               CINTER = (VELCTY-R3ERLY)/(R3LATE-R3ERLY)
83               FINTER = CINTER*RANGE1 + TABLE(JJ-1,KK-1)
84               SINTER = CINTER*RANGE2 + TABLE(JJ,KK-1)
85               RANGE3 = SINTER-FINTER
86               DINTER = (RD2D1-R4ERLY)/(R4LATE-R4ERLY)
87               ALOSSC(K) = DINTER*RANGE3 + FINTER
88               GO TO 550
89      561      CNLOSS = 0.582 + 0.0418/(1.1-DIAM/CHDIAM)
90               ALOSSC(K) = (1/CNLOSS-1)**2
91      550  CONTINUE
92           RETURN
93           END
94      C
95      C
96      C  THE FOLLOWING SUBROUTINE COMPUTES THE END-DEPTH FOR IN
97      C  THE DRILL-DROP UPPER CHAMBER USING THE WEIR FLOW EQUATION
98      C  DEVELOPED IN THE REPORT.
99      C
100     C
101          SUBROUTINE ENDPTH
102          COMMON DIAM, ENDPH(20), QDROP(20), AINIYE, GRAVTY, CHDIAM
103            PIE = 3.14159265/12.
104            ACONST = SIN(PIE)**2
105            BCONST = 2.*ACONST
106            YRATIO = 0.725
107            CCONST = 2./3.*ACONST*( 1. + YRATIO + YRATIO**2 )
108            CONST5 = 16. * ( BCONST-CCONST )
109            CONST4 = 8.*BCONST - 4.*CCONST
110            CONST3 = BCONST
111            YENDR  = AINIYE/(DIAM/2.)
112            X      = 12.
113     C
114     C
115     C  THE FOLLOWING DO LOOP COMPUTES THE END-DEPTHS FOR 20 DIFFERENT
116     C  DISCHARGES. NEWTON-RALPHSON TECHNIQUE IS USED TO SOLVE FOR
117     C  YENDR.
118     C
119     C
```

```
120               DO 200 I=1,20
121               KI = 21 - I
122                 DCONST =(QDROP(KI)**2/GRAVTY/(DIAM/2)**5/X**2)*YRATIO**2
123                 CONST1 = DCONST * 4.
124                 CONSTO = DCONST * 0.275
125       100       FCN =(CONST3*YENDR**3+CONST4*YENDR**4+CONST5*YENDR**5)
126           *           -(CONST1*YENDR + CONSTO)
127                 DFCN =(3.*CONST3*YENDR**2 + 4.*CONST4*YENDR**3)
128           *            +(5*CONST5*YENDR**4 - CONST1)
129                 YENDR2 = YENDR - FCN/DFCN
130                 DIFF = ABS( YENDR2-YENDR )
131                 IF ( DIFF .LT. 0.0001 ) GO TO 150
132                 YENDR = YENDR2
133                 GO TO 100
134       150       YENDR = YENDR2
135                 ENDPH(KI) = YENDR*(DIAM/2.)
136       200     CONTINUE
137             RETURN
138             END
139       C
140       C
141       C  THE FOLLOWING SUBROUTINE COMPUTES THE HEADS IN THE DRILL-DROP
142       C  UPPER CHAMBER USING THE WEIR FLOW EQUATION, THE FULL-PIPE FLOW
143       C  EQUATIONS, AS WELL AS THE CAVITATING FLOW EQUATION FOR THE
144       C  INPUT DISCHARGES.
145       C
146       C
147             SUBROUTINE HEAD
148             COMMON DIAM, ENDPH(20) , QDROP(20), AINIYE, GRAVTY, CHDIAM
149             COMMON /SUB02/HWEIR(20), HFULL(20), HCAVI(20)
150             COMMON /SUB03/ALENGT,FPRIME, PRDOWN, ALOSSC(20), ALOSSB, PRCAV
151               PIE1  = 3.14159265
152             DO 300 I=1,20
153       C
154       C  WEIR FLOW
155       C
156               YENDR = ENDPH(I)/(DIAM/2.)
157               QSTAR2 = QDROP(I)**2/GRAVTY/(DIAM/2)**5
158               HEADR = YENDR + QSTAR/8/PIE1**2/YENDR**2
159               HWEIR(I) = HEADR*DIAM/2
160       C
161       C  FULL-PIPE FLOW
162       C
163               VELCTY = QDROP(I)/PIE1/(DIAM/2.)**2
164               COEFF = 1 + FPRIME*ALENGT/DIAM + ALOSSC(I) + ALOSSB
165               VHEAD = VELCTY**2/2./GRAVTY
166               HFULL(I) = COEFF*VHEAD + PRDOWN - ALENGT
167       C
168       C  CAVITATING FLOW
169       C
170               HCAVI(I) = PRCAV + (ALOSSC(I) + 1)*VHEAD
171        300  CONTINUE
172             RETURN
173             END
174       C
175       C
176       C  THIS SUBROUTINE DETERMINE WHICH FLOW TYPE GOVERNS FOR
177       C  THE PARTICULAR DROP PIPE SIZE AND DISCHARGE.
178       C  RESULTS FOR THE RUN WILL ALSO BE PRINTED.
179       C
```

```
      C
            SUBROUTINE RESULT
            COMMON DIAM, ENDPH(20) , QDROP(20), AINIYE, GRAVTY, CHDIAM
            COMMON /SUB02/HWEIR(20), HFULL(20), HCAVI(20)
            COMMON /SUB03/ALENGT,FPRIME, PRDOWN, ALOSSC(20), ALOSSB, PRCAV
      C
      C  DETERMINE THE GOVERNING FLOW TYPE
      C
            DO 400 I=1,20
              IF (HWEIR(I).GE.HFULL(I)) GO TO 405
                IF (HFULL(I).GE.HCAVI(I)) GO TO 410
                GO TO 415
       405        IF (HWEIR(I).GE.HCAVI(I)) GO TO 420
       415      HACTUL = HCAVI(I)
                WRITE (6,416) QDROP(I), HACTUL, ALOSSC(I)
       416      FORMAT ('O',10X,F8.2,13X,F7.2,11X,'CAVITATING',10X,F12.3)
                GO TO 400
       420        HACTUL = HWEIR(I)
                  WRITE (6,417) QDROP(I), HACTUL
       417        FORMAT ('O',10X,F8.2,13X,F7.2,12X,'WEIR FLOW',20X,'--')
                  GO TO 400
       410    HACTUL = HFULL(I)
              WRITE (6,418) QDROP(I), HACTUL, ALOSSC(I)
       418    FORMAT ('O',10X,F8.2,13X,F7.2,12X,'FULL FLOW',10X,F12.3)
       400  CONTINUE
            RETURN
            END
      C
      C
      C  THIS SUBROUTINE READS IN THE NECESSARY DATA INTERACTIVELY
      C
      C
            SUBROUTINE READ
            COMMON DIAM, ENDPH(20), QDROP(20), AINIYE, GRAVTY, CHDIAM
            COMMON /SUB03/ALENGT,FPRIME, PRDOWN, ALOSSC(20), ALOSSB, PRCAV
            COMMON /SUB04/AMANN, IUNIT, QMAX, QMIN, ISTART
            WRITE (7,101)
       101  FORMAT ('THIS IS A PROGRAM DESIGNED TO ANALYZE DRILL DROP',/
           *'SIZE AND CAPACITY. IT IS DESIGNED TO HAVE ALL THE DATA',/
           *'INPUTTED INTERACTIVELY.')
            WRITE (7,103)
       103  FORMAT ('ENTER DROP PIPE SIZE, LENGTH AND ROUGHNESS',/
           *'IN THE FORM 2*XXX.XX, X.XXXXX',/
           *'OR HIT BREAK TO TERMINATE THE RUN')
            READ (7,104) DIAM, ALENGT, AMANN
       104  FORMAT (2F6.2, F7.5)
            WRITE (7,105)
       105  FORMAT ('ENTER HEAD CHAMBER DIAMETER, XXX.XX')
            READ (7,106) CHDIAM
       106  FORMAT (F6.2)
            WRITE (7,107)
       107  FORMAT ('ENTER BEND LOSS COEFFICIENT OR ZERO, XX.XXX')
            READ (7,108) ALOSSB
       108  FORMAT (F6.3)
            WRITE (7,102)
       102  FORMAT ('ENTER OUTLET PRESSURE HEAD, XXX.XX')
            READ (7,109) PRDOWN
       109  FORMAT (F6.2)
            WRITE (7,110)
       110  FORMAT ('ENTER MAXIMUM AND MINIMUM DISCHARGE, 2*XXXX.XX')
```

```
      READ (7,111) QMAX, QMIN
  111 FORMAT (2F7.2)
      WRITE (7,112)
  112 FORMAT ('ENTER INITIAL VALUE OF END DEPTH XXX.XX')
      READ (7,113) AINIYE
  113 FORMAT (F6.2)
      WRITE (7,114)
  114 FORMAT ('WHAT UNIT ARE YOU USING?'/ 'ENTER O FOR BRITISH,
     *1 FOR METRIC')
      READ (7,115) IUNIT
  115 FORMAT (I1)
      WRITE (7,116)
  116 FORMAT ('DO YOU WANT TO GO THROUGH WITH IT?'/
     *'ENTER O FOR GO AHEAD, 1 TO NEGATE')
      READ (7,117) ISTART
  117 FORMAT (I1)
      RETURN
      END
C
C
C  THIS SUBROUTINE DETERMINE THE TYPE OF UNIT TO BE USED,
C  THE ARRAY OF DICHARGES WITHIN THE RANGE ENTERED, THE CAVITATING
C  PRESSURE, ALSO IT WILL CONVERT MANNING'S N INTO DARCY-WEISBACH
C  FRICTION FACTOR.
C
C
      SUBROUTINE DETRMN
      COMMON DIAM, ENDPH(20), QDROP(20), AINIYE, GRAVTY, CHDIAM
      COMMON /SUB03/ALENGT,FPRIME, PRDOWN, ALOSSC(20), ALOSSB, PRCAV
      COMMON /SUB04/AMANN, IUNIT, QMAX, QMIN, ISTART
      QINTVL = (QMAX-QMIN)/20.
      QDROP(1) = QMIN
      DO 700 I=2,20
      QDROP(I) = QDROP(I-1) + QINTVL
  700 CONTINUE
      IF (IUNIT .EQ. 1) GO TO 710
      GRAVTY = 32.2
      PRCAV = -31.
      GO TO 720
  710 GRAVTY = 9.81
      PRCAV = -9.45
  720 CONTINUE
      FPRIME = (185.*AMANN**2)/(DIAM**(1./3.))
      RETURN
      END
C
C
C  THIS SUBROUTINE WILL ECHO-CHECK INPUT DATA AND PRINT HEADINGS
C  FOR THE RESULTS.
C
C
      SUBROUTINE PRINT
      COMMON DIAM, ENDPH(20), QDROP(20), AINIYE, GRAVTY, CHDIAM
      COMMON /SUB03/ALENGT,FPRIME, PRDOWN, ALOSSC(20), ALOSSB, PRCAV
      COMMON /SUB04/AMANN, IUNIT, QMAX, QMIN, ISTART
      WRITE (6,808)
  808 FORMAT ('1',/'-',/'-')
      WRITE (6,801) DIAM, PRCAV
  801 FORMAT ('O', 9X, 'DIAMETER OF PIPE  =', F8.2,10X,
     *'CAVITATING PRESSURE =', F8.2)
```

```
      WRITE (6,802) ALENGT, ALOSSB
  802 FORMAT ('O', 9X, 'LENGTH OF DROP    =', F8.2,10X,
     *'BEND LOSS COEFF     =', F8.2)
      WRITE (6,803) AMANN, PRDOWN
  803 FORMAT ('O', 9X, 'MANNINGS N        =', F8.4,10X,
     *'OUTLET PEIZ. HEAD   =', F8.4)
      IF (IUNIT .EQ. 1) GO TO 850
      WRITE (6,804) CHDIAM
  804 FORMAT ('O', 9X, 'HEAD CHAMBER SIZE =', F8.2,10X,
     *'UNIT IS BRITISH')
      GO TO 860
  850 WRITE (6,805) CHDIAM
  805 FORMAT ('O', 9X, 'HEAD CHAMBER SIZE =', F8.2,10X,
     *'UNIT IS METRIC')
  860 WRITE (6,806)
  806 FORMAT ('O',8X,78 ('*'))
      WRITE (6,807)
  807 FORMAT ('O', 10X, 'DISCHARGE', 15X, 'HEAD', 10X,
     *'TYPE OF FLOW', 7X,'ENTRANCE LOSS COEFF')
      WRITE (6,806)
      RETURN
      END
C
C
C  THIS SUBROUTINE PRINTS THE HEADS FOR THE INPUT DISCHARGES
C  FOR WEIR FLOWS, FULL-PIPE FLOW , AND CAVITATING FLOW.
C
C
      SUBROUTINE PRINT2
      COMMON DIAM, ENDPH(20) , QDROP(20), AINIYE, GRAVTY, CHDIAM
      COMMON /SUB02/HWEIR(20), HFULL(20), HCAVI(20)
      WRITE (6,912)
      WRITE (6,911)
      WRITE (6,910)
  910 FORMAT ('O',8X,'DISCHARGE',10X,'WEIR HEAD',7X,
     *'FULL-FLOW HEAD',7X,'CAVITATING HEAD')
      WRITE (6,911)
  911 FORMAT ('O',8X,71('*'))
  912 FORMAT ('1',/'-',/'-')
      DO 920 I =1, 20
      WRITE (6,913) QDROP(I), HWEIR(I), HFULL(I), HCAVI(I)
  913 FORMAT ('O',8X,F9.2,10X,F9.2,7X,F14.2,7X,F15.2)
  920 CONTINUE
      RETURN
      END
End of file
```

DIAMETER OF PIPE =	1.00	CAVITATING PRESSURE =	-31.00
LENGTH OF DROP =	100.00	BEND LOSS COEFF =	0.0
MANNINGS N =	0.0130	OUTLET PEIZ. HEAD =	0.0
HEAD CHAMBER SIZE =	4.00	UNIT IS BRITISH	

DISCHARGE	HEAD	TYPE OF FLOW	ENTRANCE LOSS COEFF
100.00	1024.72	FULL FLOW	0.341
95.00	915.06	FULL FLOW	0.341
90.00	811.02	FULL FLOW	0.341
85.00	712.61	FULL FLOW	0.341
80.00	619.82	FULL FLOW	0.341
75.00	532.65	FULL FLOW	0.341
70.00	451.11	FULL FLOW	0.341
65.00	375.19	FULL FLOW	0.341
60.00	304.90	FULL FLOW	0.341
55.00	240.23	FULL FLOW	0.341
50.00	181.18	FULL FLOW	0.341
45.00	127.76	FULL FLOW	0.341
40.00	79.95	FULL FLOW	0.341
35.00	37.78	FULL FLOW	0.341
30.00	1.31	FULL FLOW	0.345
25.00	0.89	WEIR FLOW	--
20.00	0.78	WEIR FLOW	--
15.00	0.66	WEIR FLOW	--
10.00	0.52	WEIR FLOW	--
5.00	0.34	WEIR FLOW	--

DISCHARGE	WEIR HEAD	FULL-FLOW HEAD	CAVITATING HEAD
100.00	1.89	1024.72	306.68
95.00	1.84	915.06	273.76
90.00	1.79	811.02	242.52
85.00	1.73	712.61	212.98
80.00	1.68	619.82	185.12
75.00	1.62	532.65	158.95
70.00	1.56	451.11	134.47
65.00	1.50	375.19	111.67
60.00	1.44	304.90	90.57
55.00	1.37	240.23	71.15
50.00	1.30	181.18	53.42
45.00	1.23	127.76	37.38
40.00	1.15	79.95	23.03
35.00	1.07	37.78	10.37
30.00	0.98	1.31	-0.52
25.00	0.89	-29.34	-9.53
20.00	0.78	-54.54	-17.02
15.00	0.66	-74.30	-23.00
10.00	0.52	-88.54	-27.41
5.00	0.34	-97.12	-30.09